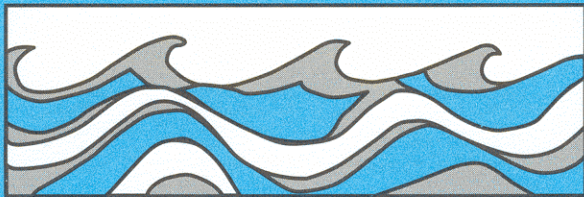


University of Washington
Department of Civil and Environmental Engineering



NUMERICAL MODELING OF TIDE AND
CIRCULATION IN CENTRAL PUGET SOUND:
COMPARISON OF A THREE-DIMENSIONAL
AND A DEPTH-AVERAGED MODEL

Wen-sen Chu
Jiing-Yih Liou
Kathleen Dillon Flenniken



Water Resources Series
Technical Report No.109
June 1988

Seattle, Washington
98195

Department of Civil Engineering
University of Washington
Seattle, Washington 98195

NUMERICAL MODELING OF TIDE AND CIRCULATION IN
CENTRAL PUGET SOUND:
COMPARISON OF A THREE-DIMENSIONAL AND A DEPTH-
AVERAGED MODEL

Wen-sen Chu
Jiing-Yih Liou
Kathleen Dillon Flenniken

Water Resources Series
Technical Report No. 109

June 1988

Numerical Modeling of Tide and Circulation in Central
Puget Sound: Comparison of a Three-Dimensional and
a Depth-Averaged Model

by

Wen-sen Chu
Jiing-Yih Liou
and
Kathleen Dillon Flenniken

Department of Civil Engineering
University of Washington
Seattle, WA 98195

Project Completion Report Submitted to
The State of Washington Water Research Center

and

The U.S. Department of the Interior
Water Research Center Project No. A-153-WASH
U.S. Department of Interior Project No. G1456-05

For the Period
April 1, 1987 to March 31, 1988

June 1988

TABLE OF CONTENTS

	Page
LIST OF FIGURES	iv
LIST OF TABLES	v
Chapter 1 INTRODUCTION	1
Chapter 2 PREVIOUS WORK	5
Chapter 3 THE THREE-DIMENSIONAL AND DEPTH-AVERAGED HYDRODYNAMIC MODELS	8
3.1 Three-Dimensional Model Governing Equations	8
3.2 Three-Dimensional Model Solution Method	13
3.3 The Depth-Averaged Model Governing Equations	16
3.4 The Depth-Averaged Model Solution Method	18
Chapter 4 MODEL APPLICATIONS	20
4.1 Study Area and Resolution	20
4.2 Boundary and Initial Conditions and Observation Data	23
4.3 Comparison with Observed Tidal Amplitude and Phase	25
4.4 Comparison with Observed Tidal Current	26
Chapter 5 SUMMARY AND CONCLUSIONS	46
REFERENCES	49

ABSTRACT

As an attempt to better understanding the tidal hydraulics and transport characteristics of Puget Sound, a depth-averaged and a three-dimensional hydrodynamics model were developed and evaluated. To limit the area of application in this initial investigation, the models were applied to a part of Puget Sound from Point Wells to the Narrow at Tacoma, referred to in this study as Central Puget Sound. The objective of the investigation was to compare the models' capabilities to characterize the tide and tidal current in this area of Puget Sound and their computational requirements.

Both models applied were shown to be capable of reproducing major observed tide and tidal current characteristics in Central Puget Sound. The study revealed that at the spatial resolution of 762m, the differences between the results of the two models are small. Typical runs of the models with the current resolution require five to twenty CPU minutes on a CRAY X/MP-48 supercomputers. For general tidal circulation and transport studies with a desired resolution of 750m or more, the use of the depth-averaged model which requires three times less computing resources is recommended. For certain engineering and planning problems around the Sound which require more detailed knowledge of the tidal current, the use of the three-dimensional model with finer spatial resolution (250m or less horizontally and 15 to 50m vertically) is suggested.

The study has shown that the increasing availability of computing power, the use of multi-dimensional hydrodynamics models for estuarine environmental decision making and basic scientific research is promising.

Key Words: Numerical models, depth-averaged model, three-dimensional model, tide, tidal current, and Puget Sound

ACKNOWLEDGEMENTS

The activities on which this report is based were financed in part by the Department of the Interior, U.S. Geological Survey, through the State of Washington Water Research Center and by a Graduate School Research Fund at the University of Washington (UW). Computing support has been provided by the National Science Foundation through a Supercomputer Initiation Grant (ECS8515798) and through the San Diego Supercomputer Center, and by the Academic Computing Services at the University of Washington. All the boundary conditions and field data used in the study were provided by Harold O. Mofjeld and J. William Lavelle of the Pacific Marine Environmental Laboratory, National Oceanic and Atmospheric Administration (PMEL/NOAA). The continuing encouragement and insight into the model results provided by Harold O. Mofjeld, J. William Lavelle, E.D. (Ned) Cokelet, Glenn Cannon, Herbert Curl, and James Holbrook all of PMEL/NOAA and Harry Yeh at the UW are greatly appreciated. Margo Behler and Kim Nguyen skillfully typed many draft versions of this report with patience and care.

LIST OF FIGURES

Figure		Page
1.1	Map of Puget Sound	2
3.1	Three-Dimensional Control Volumes	9
3.2	A Single Layer Control Volume for the Depth-Averaged Model	17
4.1	Central Puget Sound - Study Area	21
4.2	Horizontal Resolution of Central Puget Sound	22
4.3	Comparison of Calculated and Observed M_2 Tidal Amplitudes and Phases	27
4.4	Comparison of Calculated and Observed K_1 Tidal Amplitudes and Phases	28
4.5a	Comparison of Calculated and Observed M_2 Current Ellipses at MESA Station No. 2	29
4.5b	Comparison of Calculated and Observed M_2 Current Ellipses at MESA Station No. 3	30
4.5c	Comparison of Calculated and Observed M_2 Current Ellipses at MESA Station No. 5	31
4.5d	Comparison of Calculated and Observed M_2 Current Ellipses at MESA Station No. 6	32
4.5e	Comparison of Calculated and Observed M_2 Current Ellipses at MESA Station No. 7	33
4.6a	Comparison of Calculated and Observed K_1 Current Ellipses at MESA Station No. 2	34
4.6b	Comparison of Calculated and Observed K_1 Current Ellipses at MESA Station No. 3	35
4.6c	Comparison of Calculated and Observed K_1 Current Ellipses at MESA Station No. 5	36
4.6d	Comparison of Calculated and Observed K_1 Current Ellipses at MESA Station No. 6	37
4.6e	Comparison of Calculated and Observed K_1 Current Ellipses at MESA Station No. 7	38
4.7	First Layer M_2 Residual Circulation Around Vashon Island Calculated from Three-Dimensional Model Results	41
4.8	Selected Sections Around Vashon Island for Residual Circulation Calculation	43

LIST OF TABLES

Table		Page
4.1	Cross-Sectionally Averaged M_2 Residual Current Around Vashon Island Calculated from the Three-Dimensional Model Results	44
4.2	Cross-Sectionally Averaged M_2 Residual Current Around Vashon Island Calculated from the Depth-Averaged Model Results	45

CHAPTER 1

INTRODUCTION

Puget Sound (Fig. 1.1), located in the northwest corner of the United States continent, is a glaciated fjord-like estuary formed roughly thirteen thousand years ago (Burns, 1985). The complex bathymetry of the Sound is characterized by several deep basins with maximum depths exceeding 250m) separated by shallow sills (with depths vary from 40 to 60m).

The protected water of the Sound has been subject to increased urban and industrial development, marine transportation, commercial fishing, and recreational activities. The Sound presently is the receiving water for some 400 permitted industrial facilities and municipal sewage treatment plants discharging 650 million gallons daily, as well as several maintenance dredge spoils disposal sites (Puget Sound Water Quality Authority, 1987).

The perception of Puget Sound water as immaculate has changed in the last five years with reports of diseased fish and shellfish, potential health hazards from domestic sewage and industrial waste discharges, contaminated bottom sediments, and the inclusion of Commencement Bay in the U.S. Environmental Protection Agency (EPA) Superfund Project. While the contamination of Puget Sound has been recognized in recent years and a significant amount of data has been collected by several agencies, detailed spatial understanding of the Sound's circulation and transport characteristics at tidal time scale remains limited.

One of the most essential elements in managing Puget Sound water quality is the development of quantitative methods to characterize the tidal circulation and transport characteristics of the waters in Puget Sound. Numerical modeling is perhaps the most promising method at present to provide such information to the decision maker. The objective of the research on

PUGET SOUND

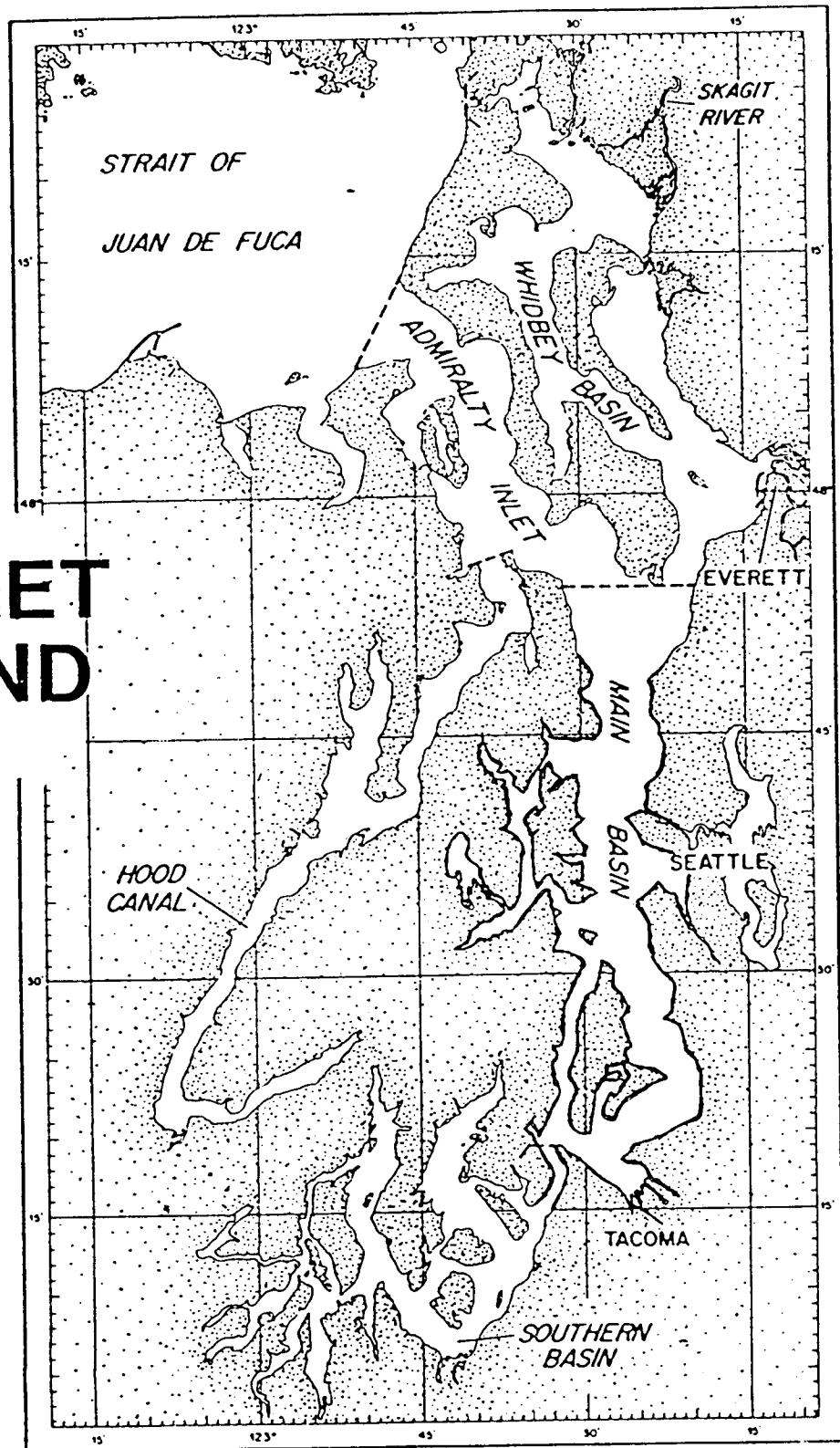


Figure 1.1 Map of Puget Sound

which this report is based was to evaluate the performance of a depth-averaged and a three-dimensional layered tidal hydrodynamics model for future applications to Puget Sound. The formulation of the depth-averaged model is predicated on the assumption that the changes of current and other water properties at any point in Puget Sound is small. While such an assumption is reasonable for the flow physics in some deeper parts of the basin, it may not be valid for other regions such as the sill zones in the Sound (Geyer and Cannon, 1982; Mofjeld and Larsen, 1984). The depth homogeneity assumption does however result in simpler model formulations and therefore smaller computing requirements. A three-dimensional model on the other hand can incorporate variations in current density structures with water depth. Three-dimensional models have the potential for more detailed characterization of the tidal current and transport, but the use of such models requires more computing resources and more boundary condition and validation data.

A particular depth-averaged and a three-dimensional model were evaluated in this study by comparing and contrasting their responses with available tide and tidal current observations. Such a comparison, which has never been attempted for Puget Sound (and rarely for other estuaries), was to the operational assess requirements, the differences, and the suitabilities of these two types of models for various decision making problems. Such information can be useful in the future selection of more appropriate models for different Puget Sound water quality management objectives.

Due to computational demands and limited data availability, the models were only implemented for part of Puget Sound from Point Wells to the Narrow in Tacoma. Central within the modeled area, tide and tidal currents were calculated by both models over several thousands of grid cells, each with a square dimension of 762 m by 762 m. The three-dimensional model further

resolved the water body into two variable thickness layers (to be elaborated later). Due partly to the goal of conserving computing resources and partly to the lack of compatible boundary condition and calibration data, density variation and wind stress are both ignored in the present modeling attempt.

An estuarine numerical model is based on mathematical formulations which approximate the behaviors of an estuarine system. The ability of the model to properly characterize the flow features of the estuary depends on the simplifying assumptions in the formulation, the resolution, the solution algorithm in the model, the available boundary condition and validation data, and to some extent, the model users (Chu, 1988). At a fixed resolution grid scale, all the flow physics smaller than the scale will have to be either parameterized (represented by some physical parameters or the resolvable flow variables) or ignored. With the chosen grid scale of 762m for the study area, the proposed models were intended for general characterization of the major current and transport features only. It should be noted here that for certain engineering, management, and research problems where more detailed information of the flow processes are required, substantial refinements of both model formulation and resolution may be required.

In the rest of the report, previous Puget Sound modeling work are reviewed in Chapter 2. The proposed three-dimensional model and the depth-averaged model are introduced in Chapter 3. Model applications and the comparison of model results with available field data are presented in Chapter 4. Findings from this study are summarized in the last chapter.

CHAPTER 2

PREVIOUS WORK

Numerical models have been widely used by oceanographers and coastal engineers. For a review of some present application of these models, the reader is referred to the recent work by Fischer (1981), Heaps (1987), Chu (1988), and Lakhan and Trenhaile (1988), and the recent issues of various leading journals in the fields of oceanography and hydraulic and coastal engineering. Our review here will concentrate only on the application of different numerical models in research and practices relating to the circulation and transport in Puget Sound.

Research on the physical oceanography of Puget Sound has been ongoing for many years (e.g. Collias, et al., 1974, Mofjeld, et al., 1987). Most of the research up to about 1984 can be classified as analytical studies from observational data (see for example, Cannon, et al., 1970; Geyer and Canon, 1982; Mofjeld and Larsen, 1984; and Bretschneider, et al., 1985). Numerical modeling of hydrodynamics and pollutant transport in Puget Sound began only recently.

One of the earliest documented numerical modeling studies of Puget Sound was the work conducted by Water Resources Engineers (WRE), Inc. (1975). The study used a one-dimensional link (channel) and node model to characterize the hydrodynamics and water quality of the Sound. Although the modeling system did include a fairly sophisticated water quality and ecological model, the one-dimensional approximation of the tidal hydrodynamics, especially with respect to momentum transport, is now considered too crude for many planning and engineering applications. More recently, Jamart and Winter (1978) developed a two-dimensional model using a harmonic method and finite element technique to calculate tidal flow in a part of Hood Canal, a major basin in

Puget Sound. Jamart (1983) later extended the same model to East Passage (the passage east of Vashon Island) in Puget Sound for a sewage treatment plant outfall siting study. Similarly, Downing et al., (1985) used a two-dimensional depth-averaged tide and transport model to investigate far field dilution for another sewage outfall siting study in the main basin of Puget Sound from West Point to Vashon Island. As part of the Puget Sound Dredge Disposal Analysis (PSDDA) program, Schmalz, Jr. (1986) applied another depth-averaged hydrodynamic model to Puget Sound to provide tidal current information for dredge disposal site selection. Because of the nature of the studies (objective, budget, and time limitations), these previous investigations all used only two-dimensional models. For the concerns related to outfall and dredge disposal site selections, more refined tidal current information might need to be considered. Such information can be provided by a three-dimensional model with refined resolution.

The application of the three-dimensional models in Puget Sound should first be examined by comparing their performances with existing observational data.

Other more recently developed models include a one-dimensional channel tide model for calculating tide and tidal transport Puget Sound (Mofjeld, 1987); a laterally-averaged model for the characterization of salt water intrusion into the main basin of Puget Sound (Lavelle, 1987), and a mass conservation based "box model" for studying long term basin wide flushing characteristics of Puget Sound (Cokelet, et al., 1984). All three of these models were developed as research tools at Pacific Marine Environmental Laboratory, National Oceanic and Atmospheric Administration (PMEL/NOAA). All three models have been calibrated by extensive Puget Sound observational data available at PMEL/NOAA. To evaluate the computational characteristics of a

recently developed code, Nakata in Japan (1987) applied his three-dimensional model to an "idealized Puget Sound basin" assuming a uniform depth throughout the Sound. No rigorous validation of the model was attempted.

Two of the above cited previous works are of significant importance to this study. The compiled and analyzed tide and tidal current data at various stations in Puget Sound from Mofjeld and Larsen (1984) are used for model comparison purpose (see Chapter 4). The well-calibrated channel tide model by Mofjeld (1987) was used to provide boundary conditions of tidal transport (flow rate) at the boundaries of the study area. The actual implementation procedure is presented in detail in Section 4.2.

CHAPTER 3

THE THREE-DIMENSIONAL HYDRODYNAMICS MODEL

The three-dimensional model given below allows the approximation of the hydrodynamics in Puget Sound in layers of control volumes as shown in Fig.

3.1. The mass and momentum transport between the control volumes in the horizontal and vertical directions (in Cartesian x-y-z Coordinate System) are represented by a reduced form of the Reynold's Equations. The formulation and the solution algorithm are presented in the next two section.

3.1 Three-Dimensional Model Governing Equations

If we assume the water is of uniform density (well-mixed, barotropic) and if we could ignore vertical acceleration of the flow due to its small magnitude relative to gravitational acceleration, then the tidal hydrodynamics in Puget Sound can be described with respect to a control volume in a middle (K^{th}) layer (see Fig. 3.1) by:

$$\begin{aligned} \frac{\partial(hu)}{\partial t} + \frac{\partial(huu)}{\partial x} + \frac{\partial(huv)}{\partial y} + (wu)_{K-1/2} - (wu)_{K+1/2} - fhv + \frac{h}{\rho} \frac{\partial p}{\partial x} - \left(\frac{1}{\rho} \tau^{xz}\right)_{K-1/2} \\ + \left(\frac{1}{\rho} \tau^{xz}\right)_{K+1/2} - \frac{1}{\rho} \frac{\partial}{\partial x} \left(hA \frac{\partial u}{\partial x}\right) - \frac{1}{\rho} \frac{\partial}{\partial y} \left(hA \frac{\partial u}{\partial y}\right) = 0 \end{aligned} \quad (3.1)$$

$$\begin{aligned} \frac{\partial(hv)}{\partial t} + \frac{\partial(huv)}{\partial x} + \frac{\partial(hvv)}{\partial y} + (wv)_{K-1/2} - (wv)_{K+1/2} + fhu + \frac{h}{\rho} \frac{\partial p}{\partial y} - \left(\frac{1}{\rho} \tau^{yz}\right)_{K-1/2} \\ + \left(\frac{1}{\rho} \tau^{yz}\right)_{K+1/2} - \frac{1}{\rho} \frac{\partial}{\partial x} \left(hA \frac{\partial v}{\partial x}\right) - \frac{1}{\rho} \frac{\partial}{\partial y} \left(hA \frac{\partial v}{\partial y}\right) = 0 \end{aligned} \quad (3.2)$$

$$w_{K-1/2} - w_{K+1/2} = - \frac{\partial(hu)}{\partial x} - \frac{\partial(hv)}{\partial y} \quad (3.3)$$

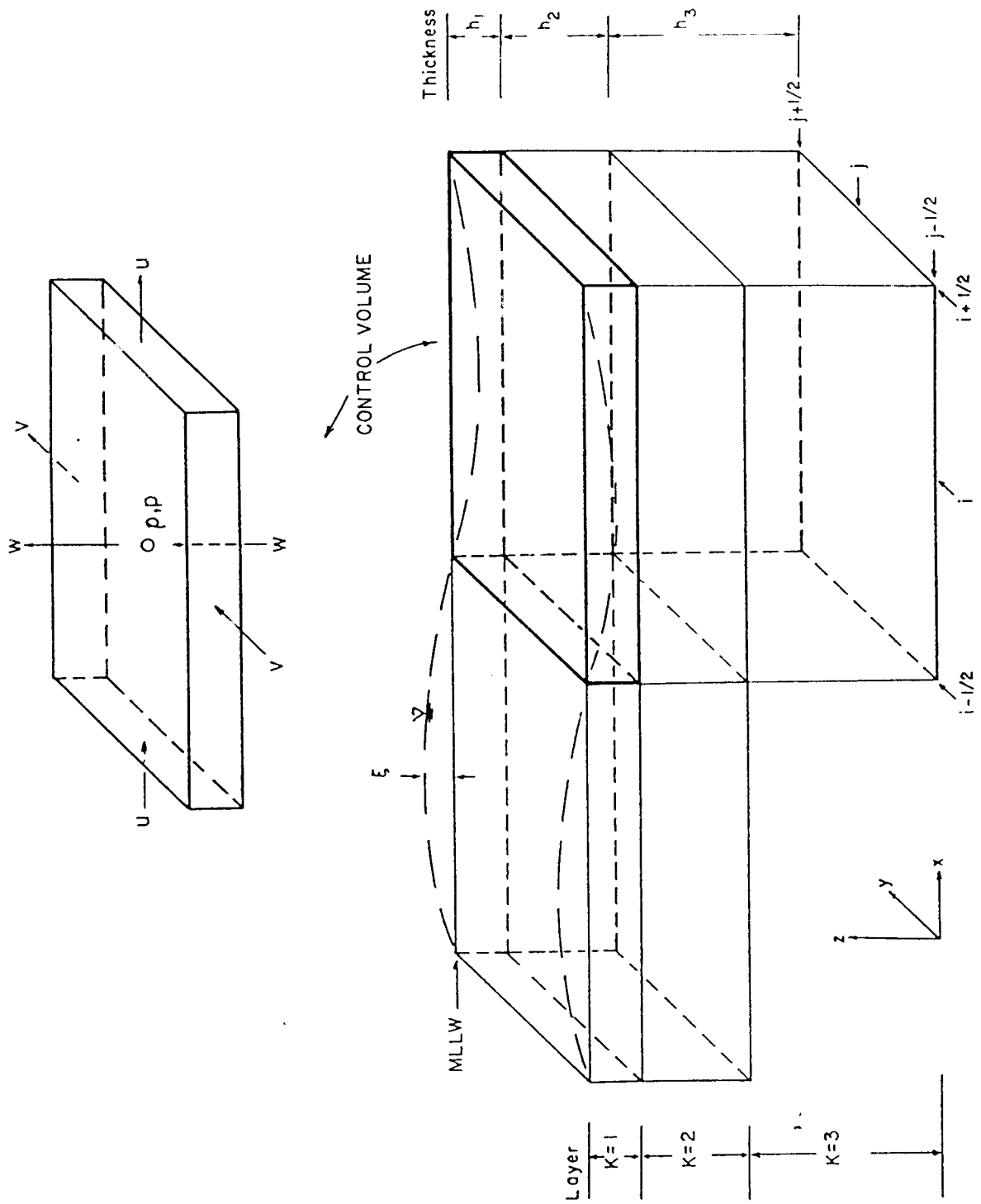


Figure 3.1 Three-Dimensional Control Volumes

where u and v are the layer-averaged horizontal velocities in x - and y -directions, w is the vertical velocity, h is layer thickness which can vary according to particular chosen vertical resolution (see Fig. 3.1), p is hydrostatic pressure, ρ is water density, τ^{xZ} and τ^{yZ} are the x - and y -component turbulent shear stresses between two vertical layers, the last two terms in Eqs. (3.1) and (3.2) are turbulent shear stresses between two adjacent control volumes in the horizontal directions, f is the Coriolis parameter, and A is the horizontal momentum exchange coefficient.

In this model, the horizontal momentum exchange coefficient is expressed as (Leendertse and Liu, 1978):

$$A = \gamma \left| \frac{\partial \omega}{\partial x} + \frac{\partial \omega}{\partial y} \right| (\Delta L)^3 \quad (3.4)$$

where γ is a constant, ω is the z -component vorticity ($\omega = \frac{\partial v}{\partial x} - \frac{\partial u}{\partial y}$), and ΔL is the horizontal dimension of the control volume, which is also the minimum size of eddies resolvable by the model.

The vertical momentum exchange process in the K^{th} layer is represented in the model by:

$$- \left(\frac{1}{\rho} \tau^{xZ} \right)_{K-1/2} + \left(\frac{1}{\rho} \tau^{xZ} \right)_{K+1/2} = - \left(E \frac{\partial u}{\partial z} \right)_{K-1/2} + \left(E \frac{\partial u}{\partial z} \right)_{K+1/2} \quad (3.5)$$

$$- \left(\frac{1}{\rho} \tau^{yZ} \right)_{K-1/2} + \left(\frac{1}{\rho} \tau^{yZ} \right)_{K+1/2} = - \left(E \frac{\partial v}{\partial z} \right)_{K-1/2} + \left(E \frac{\partial v}{\partial z} \right)_{K+1/2} \quad (3.6)$$

where E is the vertical momentum exchange coefficient by:

$$E = \nu \left| \frac{\partial \mathbf{V}}{\partial z} \right| \quad (3.7)$$

in which $\mathbf{V} = ui + vj$, $\nu = L^2$, and L is defined by a simple linear relationship suggested by Perrels and Karelse (1981):

$$L = \begin{cases} KZ & \text{if } Z \leq Z_d \\ KZ_d & \text{if } Z > Z_d \end{cases} \quad (3.8)$$

where Z is the local depth measure from the bottom, Z_d is taken as one-fifth of the total depth, and K is a constant. Both K and γ (Eq. 3.4) must be selected for application to particular estuaries.

Equations (3.1) and (3.2) are x- and y-component of the momentum equation, and Eq. (3.3) is the fluid continuity equation. The momentum and continuity equations for the top and bottom layers differ slightly from Eqs. (3.1), (3.2), and (3.3). For the top layer, the continuity equation becomes:

$$\frac{\partial \xi}{\partial t} + \sum_{k=1}^b \left\{ \frac{\partial(hu)}{\partial x} + \frac{\partial(hv)}{\partial y} \right\}_k = 0 \quad (3.9)$$

where ξ is the free surface elevation, with respect to a coastal datum plane, and b is the total number of layers in any column of water.

In the top layer, the shear stress terms $\left(\frac{1}{\rho} \tau^{xz}\right)_{K-1/2}$ and $\left(\frac{1}{\rho} \tau^{yz}\right)_{K-1/2}$ in Eqs. (3.1) and (3.2) are replaced by wind shear stresses as:

$$\left(\frac{1}{\rho} \tau^{xz}\right)_{K-1/2} = \frac{\rho_a}{\rho} C^* W^2 \sin\theta \quad (3.10)$$

in the top layer

$$\left(\frac{1}{\rho} \tau^{yz}\right)_{K-1/2} = \frac{\rho_a}{\rho} C^* W^2 \cos\theta \quad (3.11)$$

in the top layer

where ρ_a is the atmospheric density, W is the 10-meter wind speed, θ is the angle between wind direction and model y -axis, and C^* is the wind drag coefficient.

For the bottom layer, the shear stresses terms $(\frac{1}{\rho}\tau^{xz})_{K+1/2}$ and $(\frac{1}{\rho}\tau^{yz})_{K+1/2}$ in Equations (3.1) and (3.2) will be replaced by:

$$\left(\frac{1}{\rho}\tau^{xz}\right)_{K+1/2} = g \frac{u (u^2 + v^2)^{1/2}}{C^2} \quad (3.12)$$

in the bottom layer

$$\left(\frac{1}{\rho}\tau^{yz}\right)_{K+1/2} = g \frac{v (u^2 + v^2)^{1/2}}{C^2} \quad (3.13)$$

in the bottom layer

where C is bottom roughness parameter that also needs to be selected for particular applications.

Pressure gradient terms $\frac{\partial p}{\partial x}$ and $\frac{\partial p}{\partial y}$ in Eqs. (3.1) and (3.2) are calculated by:

$$\left. \begin{aligned} \frac{\partial p}{\partial x} &= g\rho \frac{\partial \xi}{\partial x} \\ \frac{\partial p}{\partial y} &= g\rho \frac{\partial \xi}{\partial y} \end{aligned} \right\} \quad (3.14)$$

and since the water is assumed to be homogeneous, the pressure gradients at subsequent layers will be the same.

The unknowns functions to be solved in this model are the velocity components u , v , w , the water surface elevation ξ , and the pressure gradients. These unknowns may be obtained only by numerical solution schemes. The particular solution approach adopted is introduced next.

3.2 Three Dimensional Model Solution Method

The governing equations in the above section are solved by an explicit (leapfrog) mass and momentum conservative finite difference method introduced by Leendertse et al. (1973). The complete finite difference equations and the integration procedure are given in detail in Leendertse et al. (1973), and will be omitted here for brevity.

Because of its minimal numerical damping property, the proposed leapfrog scheme is one of the most desirable finite difference methods in computational fluid dynamics (Roache, 1976; Messinger and Arakawa, 1976). However, the leapfrog scheme is only marginally stable, especially when applied to partial differential equations containing second order derivative terms. The marginal stability makes the leapfrog scheme rather unattractive when long-term simulation is required (Kurihara, 1965; Messinger and Arakawa, 1976).

One of the remedies to the stability problem is the DuFort-Frankel leapfrog scheme. But it has been shown that the DuFort-Frankel leapfrog scheme may not be significantly more stable than the regular leapfrog scheme in multi-dimensional cases (Roache, 1976). The DuFort-Frankel leapfrog scheme also requires a few more computations per time step which could significantly increase the solution time in long-term simulation. The other remedial strategy that had been suggested involves the intermittent use of other dissipative finite difference schemes during the long-term integration of a leapfrog scheme (Kurihara, 1965). Although the incorporation of any of the strategies suggested by Kurihara (1965) in the proposed model would not be difficult, they may again require a significant increase in computing requirements in long-term simulation.

Leendertse and Liu (1977) in their second three-dimensional model, reformulated the finite difference equations so that the variables are solved implicitly in the z- (vertical) direction to ensure long-term stability. Although the z-direction implicit scheme resulted in only tri-diagonal linear systems of equations, it still does not necessarily allow the use of significantly larger time steps in applications to complex water bodies. The development of a z-direction implicit code is rather difficult.

One simpler method to ensure long-term stability is the use of smoothing (filtering) operators (Richtmeyer and Morton, 1967). The smoothing schemes can be used every N (N is a user input parameter) integration steps to smooth out the undesirable higher modes of the solutions before they are amplified. Recently, a number of efficient and stable smoothing schemes have been proposed by Killworth (1984). One of the convenient smoothing schemes was adopted for the proposed three-dimensional model and is described here.

Let us assume the computation has advanced to time level $n+1$, and let Q_{n-1} , Q_n , and Q_{n+1} be vectors containing all the model solutions (velocity components, water surface elevation, pressure gradient, etc.) at time levels $n-1$, n , and $n+1$, respectively.

The smoothing operation begins by first obtaining intermediate solutions $Q_{n-1/2}$ and $Q_{n+1/2}$ which are defined as:

$$Q_{n-1/2} = \frac{1}{2} (Q_n + Q_{n-1})$$

$$Q_{n+1/2} = \frac{1}{2} (Q_{n+1} + Q_n)$$

From these intermediate values solutions, a new $Q_{n+3/2}$ is then recalculated from the model, before the solution procedure advances to the next time level.

For a one-dimensional equation, it has been shown that the above smoothing operator is stable and preserves the accuracy of the leapfrog scheme (Killworth, 1984). The smoothing procedure however creates a minor nuisance in that the solutions are no longer available at the regular time intervals once the smoothing operator is used. This problem was eliminated in this study by smoothing the solutions twice (double smoothing) each time the operator is used.

The three-dimensional model can accommodate either tide or velocities (current) as open boundary conditions along any domain boundaries. If tide is used as the boundary condition at an open boundary, then it is assumed that velocity gradient in the direction perpendicular to the open boundary is zero. If however, velocity (circulation) data is used as open boundary condition, then it is assumed that the water surface elevation gradient in the direction perpendicular to the open boundary is zero. Using the staggered grid system, the calculation at any closed boundary (assumed as a vertical wall) is handled by setting the appropriate velocity component (perpendicular to the wall) to zero. The model in the present form does not have the capability to calculate moving boundary conditions as would be observed in the drying and wetting of tide flats.

The above solution scheme and the smoothing operator were coded in FORTRAN 77. The code has been checked against an analytical solution derived for an oscillating standing wave in a rectangular tank (Leendertse et al., 1973) as well as a variety of hypothetical problems with complex boundary conditions in the last three years.

To further simplify the model structure (and therefore the computational requirements), the hydrodynamics in many estuaries and coastal waters can also be approximated by just one layer of control volume such as the kind shown in Fig. 3.2. The mass and momentum transport among the control volumes can then be represented by a further reduced set of equations written in terms of depth-averaged velocities. The basic equations for this type of model and the solution method used are introduced in the next two sections.

3.3 Depth-Averaged Model Governing Equations

If we could further assume that the vertical variation of current (and density, if it is not constant) in the water column is negligible, then the entire set of equations for the three-dimensional model can be integrated over the depth of water and expressed in terms of depth-averaged flow variables as (Liu and Leendertse, 1978; Chu and Yeh, 1985):

$$\frac{\partial U}{\partial t} + U \frac{\partial U}{\partial x} + V \frac{\partial U}{\partial y} + g \frac{\partial \xi}{\partial x} - fV - \frac{1}{\rho H} \tau_x^W + g \frac{U(U^2 + V^2)^{1/2}}{C^2 H} = 0 \quad (3.15)$$

$$\frac{\partial V}{\partial t} + U \frac{\partial V}{\partial x} + V \frac{\partial V}{\partial y} + g \frac{\partial \xi}{\partial y} + fU - \frac{1}{\rho H} \tau_y^W + g \frac{V(U^2 + V^2)^{1/2}}{C^2 H} = 0 \quad (3.16)$$

$$\frac{\partial \xi}{\partial t} + \frac{\partial(HU)}{\partial x} + \frac{\partial(HV)}{\partial y} = 0 \quad (3.17)$$

where (see Fig. 3.2) $U(x,y,t)$ and $V(x,y,t)$ are depth averaged velocity components in the x- and y-direction, $\xi(x,y,t)$ is the water surface elevation with respect to a coastal datum plane, τ_x^W , τ_y^W are wind stresses in the x- and y-direction, $H(x,y,t)$ is total water depth, g is gravitational acceleration, ρ is water density, f is the Coriolis parameter, and C is a

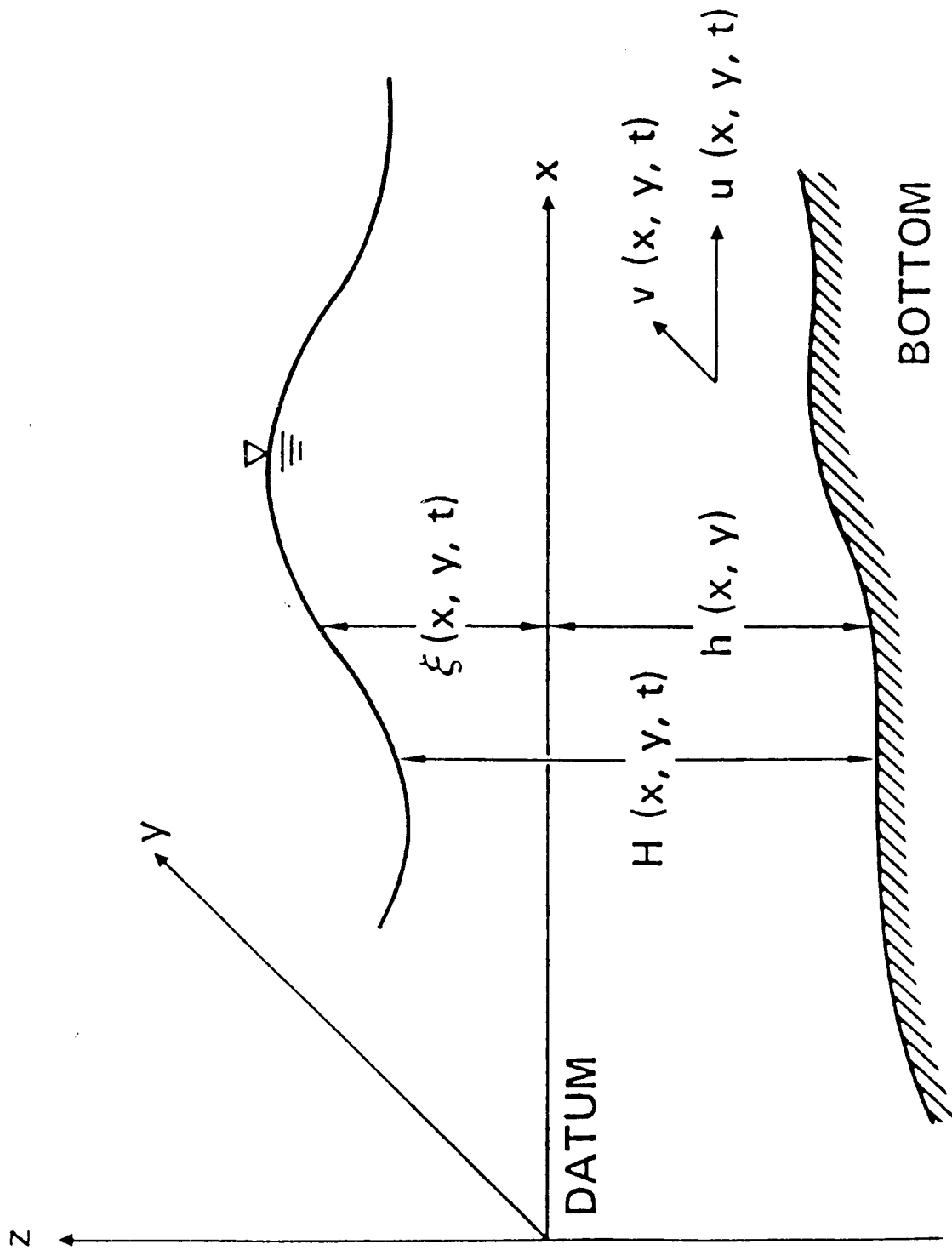


Figure 3.2 A Single Layer Control Volume for the Depth-Averaged Model

lumped roughness parameter representing both bottom roughness and other momentum exchange effects (Chu and Yeh, 1985; Yeh, et al, 1988).

Because of the averaging over the depth, this type of model is often referred to as a vertically-averaged model. The use of such a model is often justified by the "nearly-horizontal flow condition" (Abbott, et al., 1985) assumed for estuaries and coastal seas having large length to depth ratios. Such assumption typically lead to the approximation of estuarine and coastal flow physics by finite control volume (grids) having large horizontal to vertical dimension ratios. In Puget Sound (which is one of the deepest estuaries in North America) for example, the length from Admiralty Inlet to The Narrows at Tacoma is approximately 110 km while the maximum depth in the section is about 300 m, giving a minimum length to depth ratio of 367 to 1. For this reason, a depth-averaged model was considered for this study. The main objective of this study as stated earlier in this report, therefore, is to examine the validity and the computational efficiency of this depth-averaged model versus the above layered three-dimensional model for characterization of major tidal transport features in the central Puget Sound.

3.4. Depth-Averaged Model Solution Method

Using a two-dimensional equivalent of the three-dimensional staggered grid system (which can be obtained by making a projection of the grid shown in Fig. 3.1 onto a horizontal plane), the governing equations in this model are solved by the original Leendertse's semi-implicit, multi-operational finite difference scheme. This particular scheme is one of the most widely used finite difference methods in estuarine models. Since the original development, several modified versions of the idea are now available (see Leendertse, et al., 1981; Smith and Cheng, 1987). For the above formulation, this semi-implicit scheme is one of the most stable finite difference solution

methods available. But because the scheme is only semi-implicit, it is still only conditionally stable, especially for practical applications involving complex bathymetry. Detailed description of the entire finite difference equations and the solution procedure can be found in, Dronkers (1975) Liu and Leendertse (1978), and Chu, et al. (1981) and will not be repeated here.

Because of the identical staggered finite difference grid used, computations in the depth-averaged model at the open and no-flow boundaries use the same assumptions and rules defined in Section 3.2 for the three-dimensional model. The present depth-averaged model does not handle the moving boundary condition over the tide flats either.

The solution method was coded in FORTRAN. The original code has been checked against available analytical solutions, hydraulic model observations (Chu, et al., 1981), laboratory experimental data (Yeh, et al., 1988), and applied to a number of estuaries and coastal seas (Chu and Yeh, 1985; Chu, et al., 1988). The solution scheme has been found to be more stable than other explicit finite difference methods and the model can characterize large scale (scale on the order of the sizes of the finite difference grid used in those studies) flow phenomena, in general, quite satisfactorily.

CHAPTER 4

MODEL APPLICATION

Both the three-dimensional and the depth-averaged models were implemented for the same area in Puget Sound with identical boundary conditions and resolution scale. In this chapter, the study area, the boundary conditions used, and the available field observations are first introduced followed by the comparison of model results with available field observation.

4.1 Study Area and Resolution

The region in Puget Sound chosen for the modeling study is part of the main basin from Point Wells to the Narrows at Tacoma, referred to in the study as the Central Puget Sound (Fig. 4.1). This particular area was selected for three main reasons. First of all, the region covers the major population centers and some of the most polluted urban embayments in Puget Sound. Secondly, a relatively large amount of existing data were available at several oceanographic stations. Thirdly, the northern and southern boundaries (Point Wells and the Narrows) of the study area coincide with two of the cross-sections used in the channel tide model by Mofjeld (1987), at which the calculated tidal transports (flow rates) from the channel tide model were used as boundary conditions for the two models (see next section).

Using a 762m by 762m square finite difference grid, the central Puget Sound area was schematized and represented by the models as shown in Fig. 4.2. To minimize the number of dry nodes (nodes that cover dry land or islands) and to provide the best resolution of the essential geometric features with this orthogonal grid system, the model area was rotated 10 degrees counterclockwise from the magnetic north on see National Ocean Survey Chart No. 18440. Except

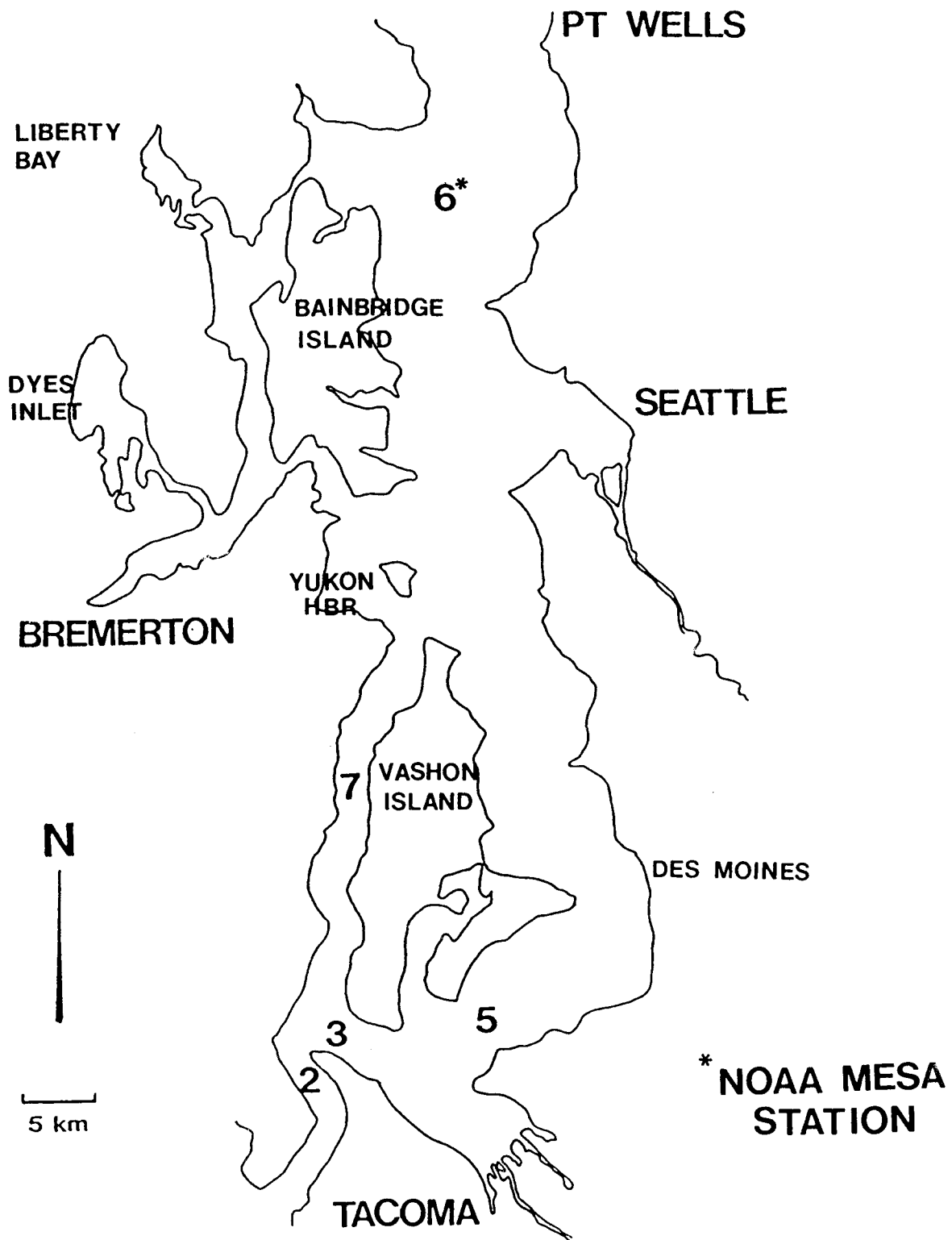


Figure 4.1 Central Puget Sound - Study Area

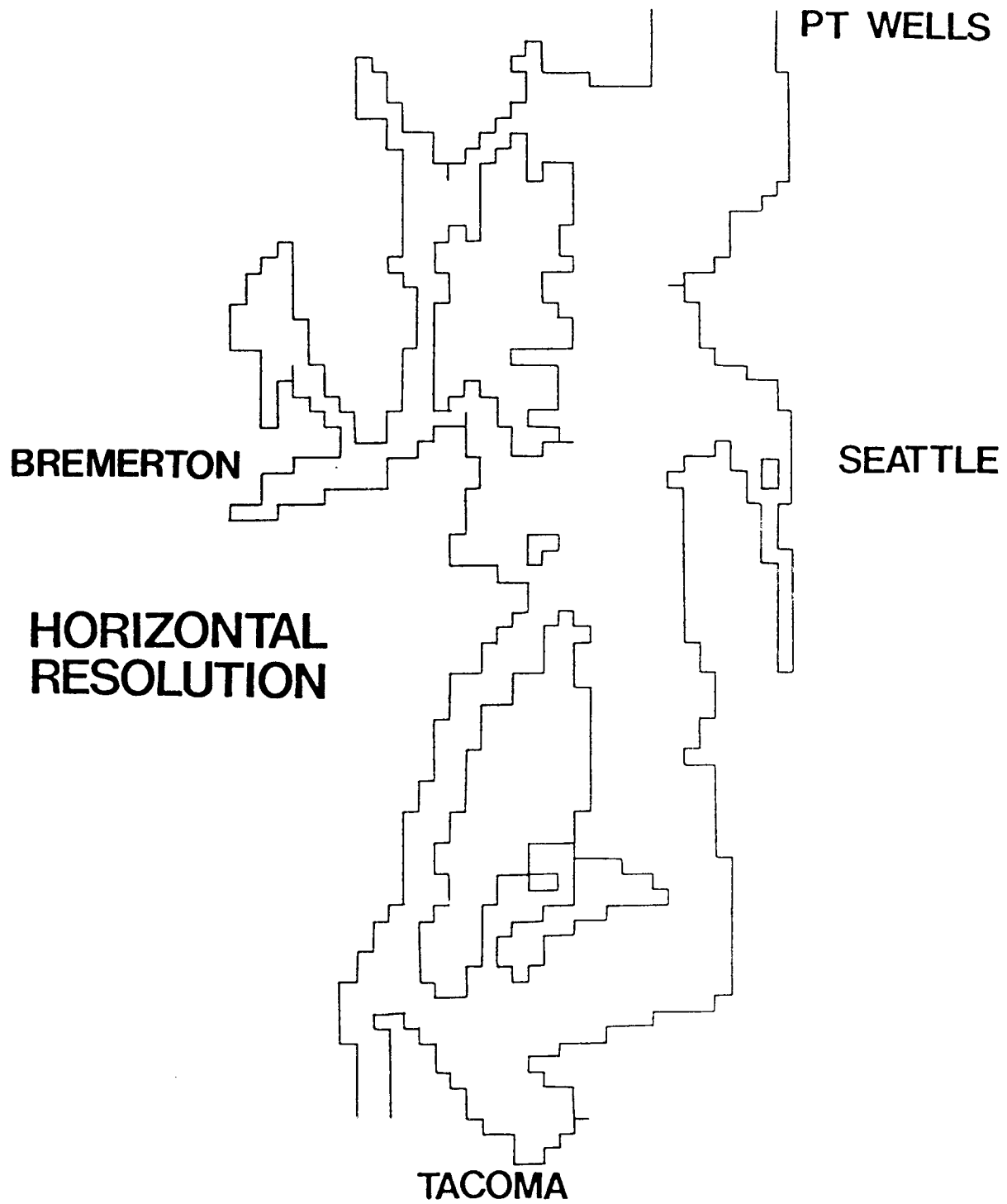


Figure 4.2 Horizontal Resolution of Central Puget Sound

for some narrow channels and the west side of the study area and the river channels, the chosen resolution captures most of the essential geometric features of Central Puget Sound. The effect of the resolution on currents in the narrow passages will be discussed later in this chapter.

Bathymetric information at all the grid nodes for the models were interpolated from data points on National Ocean Survey's Chart No. 18440. The interpolated nodal bathymetry data were entered directly in the depth-averaged two-dimensional model. The three-dimensional model instead, resolved the bathymetry in two variable thickness layers. The first layer has a variable thickness of 60m or less (the layer bottom follows the bottom of the portions with depth less than 60m). The second layer resolved the deeper portion of Central Puget Sound with a variable thickness that follows the Sound's bottom bathymetry.

Integration time step used by the three-dimensional model was six seconds, and the one used by the depth-averaged model was 12 seconds. The particular time steps were determined from the chosen spatial grid size and the maximum depth by an empirical stability equation and trial simulation runs.

4.2 Boundary and Initial Conditions and Observational Data

Because most of the present data were not collected for the purpose of numerical modeling, boundary conditions for modeling Central Puget Sound (or any other portion of the Sound) simply do not exist. For this study, the boundary conditions were obtained from a channel tide model developed at Pacific Marine Environmental Laboratory, National Oceanic and Atmospheric Administration (PMEL/NOAA) (Mofjeld, 1987). The PMEL model divides the entire Puget Sound into a series of 79 connected one-dimensional channels. Forced by tide at the entrance (Admiralty Inlet), the water level changes within each

channel and the transport (flow rate) through the cross-sections connecting the channels are calculated from one-dimensional continuity equation. The model results have been shown to have matched the observed tidal characteristics of most major tidal constituents throughout the Sound.

The northern and southern boundaries (Point Wells and the Narrow at Tacoma) of the study area were chosen to coincide with two of the cross-sections of the channel tide model. The calculated semidiurnal (M_2) and diurnal (K_1) components (two of the most significant tidal components) transports (flow rates) at these two cross-sections were used as boundary conditions for the models in this study. To do that cross-sectionally averaged currents were obtained by dividing the flow rates by the model cross-sectional areas and entered at every boundary node. Simulations using the M_2 and the K_1 boundary conditions were run separately. All river inflows (which have negligible effect on the momentum), density variation, and wind stress were ignored in this preliminary investigation.

As initial conditions, the water level in the study area at the beginning of each simulation was assumed at mean lower low water, and the currents are assumed to be zero everywhere in the domain. Starting from such conditions, the model must be run with the same boundary conditions for eight repeated cycles (12.42 hours per cycle for the M_2 and 23.92 hours per cycle for the K_1 constituent) to eliminate the "residuum" of the initial conditions in the solution. This period of simulation is often referred to as "spin-up time." The eight tidal cycle spin-up time for this study was required mainly for tidal currents. The calculated tide settled down to the prescribed boundary conditions within four tidal cycles.

In all the three-dimensional model runs, the bottom roughness coefficient (C in Eqs. 3.12 and 3.13) was set to $60 \text{ m}^{1/2}/\text{s}$. The horizontal

momentum exchange parameter (γ in Eq. 3.4) is set at 0.5. The vertical momentum exchange parameter (K in Eq. 3.8) was set at 0.4. The roughness parameter in the depth-averaged model (C in Eqs. 3.15 and 3.16) was set at $35 \text{ m}^{1/2}/\text{s}$. This smaller roughness parameter value (which provided more momentum damping effect in the model) was necessary since the parameter is the only momentum diffusion mechanism in the depth-averaged model. It was discovered from a number of parameter sensitivity simulation runs that the three-dimensional model was relatively insensitive to the changes of roughness and momentum exchange parameters and the two-dimensional model was only mildly sensitive to the changes of its roughness parameter. Both models' responses were clearly dominated by the prescribed boundary conditions, the pressure gradient (water surface elevation changes), and the input bathymetry data.

All the observational data used for comparison purpose in this study were obtained from the report by Mofjeld and Larsen (1984). Specifically, the observed tidal amplitude and phase speed of the M_2 constituent (major semi-diurnal component) at seven stations and those of the K_1 constituent (major diurnal component) at three stations were used to compare with the calculated values from the two proposed models. Calculated M_2 and K_1 tidal currents were plotted against available current ellipses (a current ellipse at a location can be constructed from a plot of selected current vectors over a tidal cycle) data from Mofjeld and Larsen (1984) at five NOAA/MESA current stations (MESA Stands for Marine Ecosystem Analysis, which was a particular NOAA Puget Sound research project) in Central Puget Sound. The comparisons and the discussion of the results are given in the next two sections.

4.3 Comparison with Observed Tidal Amplitude and Phase

The calculated M_2 amplitudes and phases are compared with observed data at stations near Seattle, Des Moines, Tacoma, Yukon Harbor, Bremerton, Dyes

Inlet, and Liberty Bay and are shown on Fig. 4.3. For both the amplitude and phase, the depth-averaged model and the three-dimensional model produced very similar results at all stations. In general, the discrepancies between the model results and the observations were smaller at stations in the main basin. The larger differences between the observed data and calculated results near Dyes Inlet were due mainly to the poor resolution of the geometry of Port Washington Narrows leading into Dyes Inlet. Amplitude differences at most other stations are within four centimeters, and the phase differences at all other stations are all within five degrees (one degree of M_2 phase equals 2.07 minutes).

The calculated and observed K_1 amplitudes and phases are plotted on Fig. 4.4. K_1 phase data were available only at Seattle, Tacoma, and Bremerton. The differences between the calculated and the observed K_1 characteristics are much smaller than those for the M_2 component. Unlike the M_2 case, the discrepancies for this component did not appear to be affected by the grid resolution as much since the differences between the computed and observed values were almost uniform over all stations.

4.4 Comparison with Observed Tidal Currents

Tidal current ellipses derived from observations near the surface over five stations within the study area were presented by Mofjeld and Larsen (1984). To compare the model results with observations, the computed first layer tidal current from the three-dimensional model and those from the depth-averaged model were plotted against the observations in Figs. 4.5 for the M_2 constituent and in Figs. 4.6 for the K_1 constituent.

Although the matches between the computed and the observed currents are not as good as those for the tides, it should be noted that the comparisons were actually made at different depths and only approximate locations.

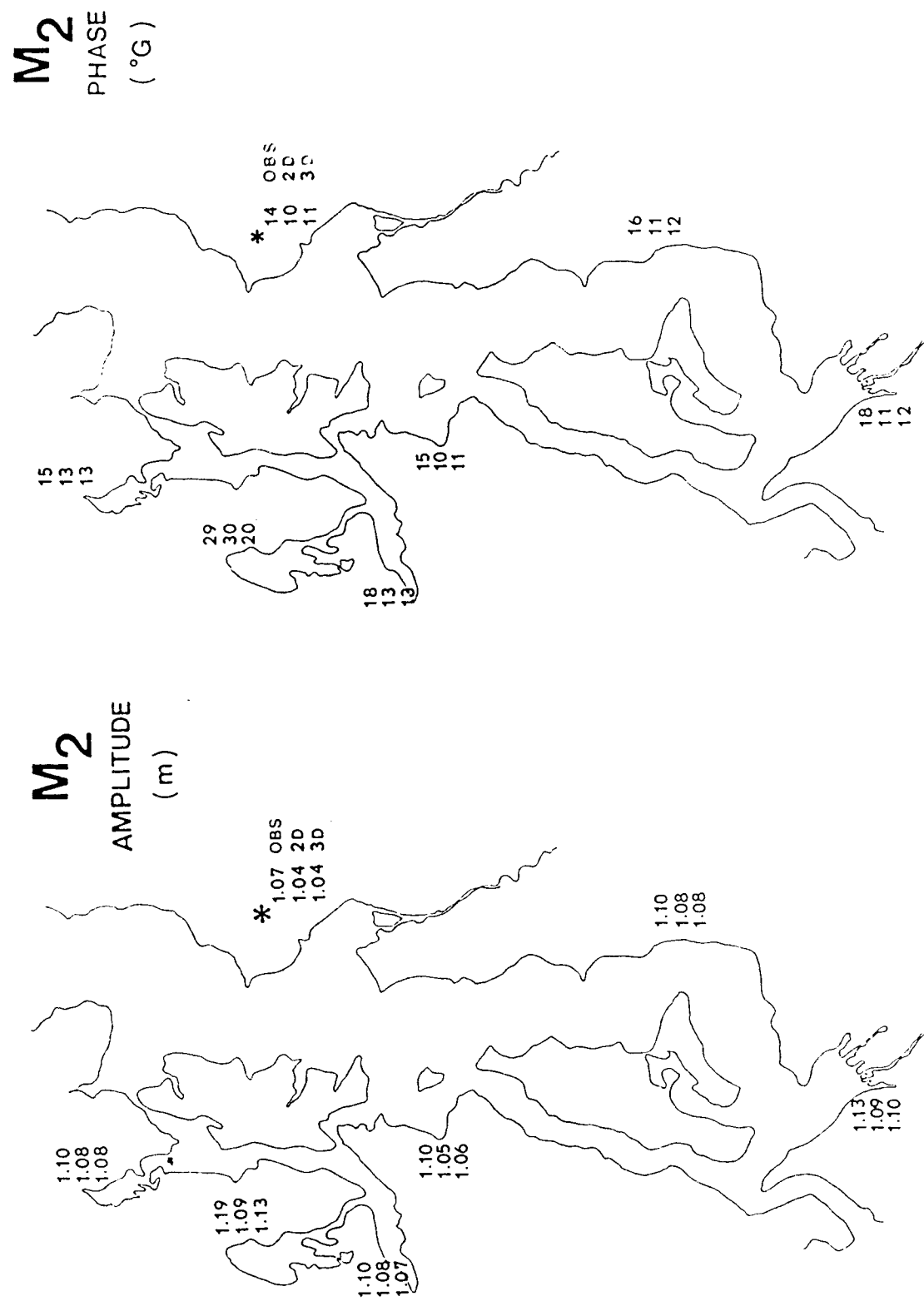
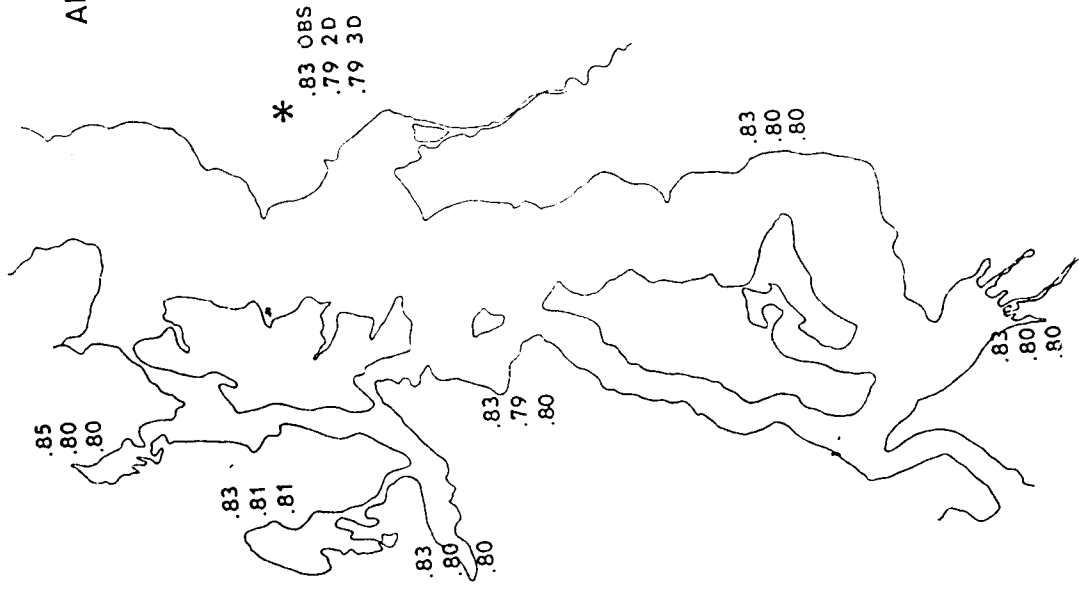


Figure 4.3 Comparison of Calculated and Observed M₂ Tidal Amplitudes and Phases

K₁
AMPLITUDE
(m)



K₁
PHASE
(°G)

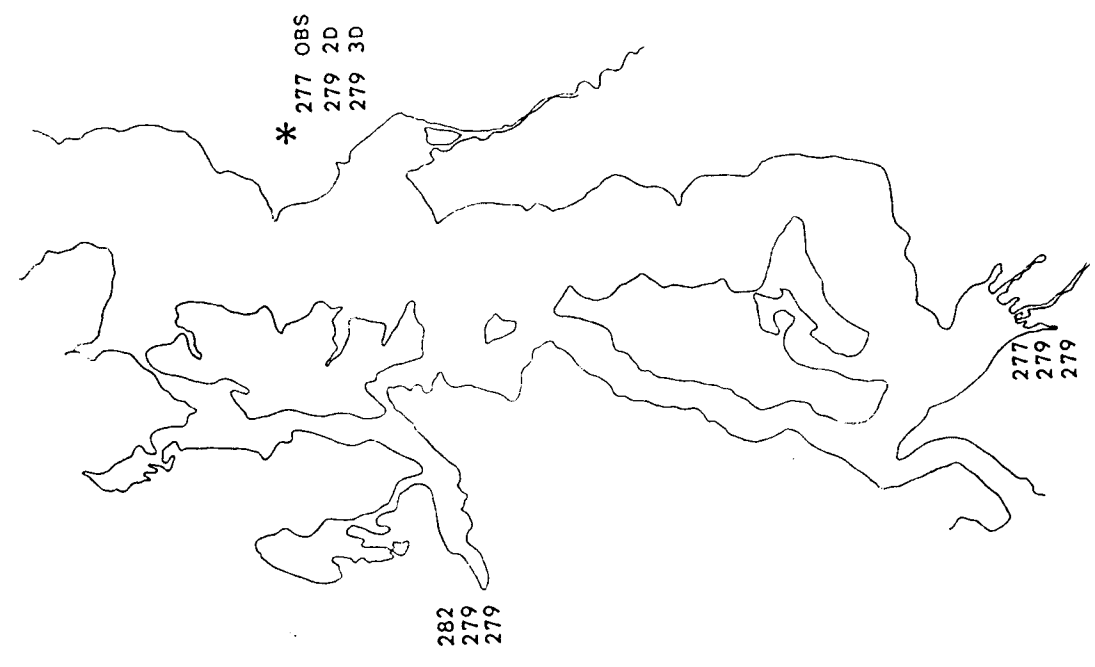


Figure 4.4 Comparison of Calculated and Observed K₁ Tidal Amplitudes and Phases

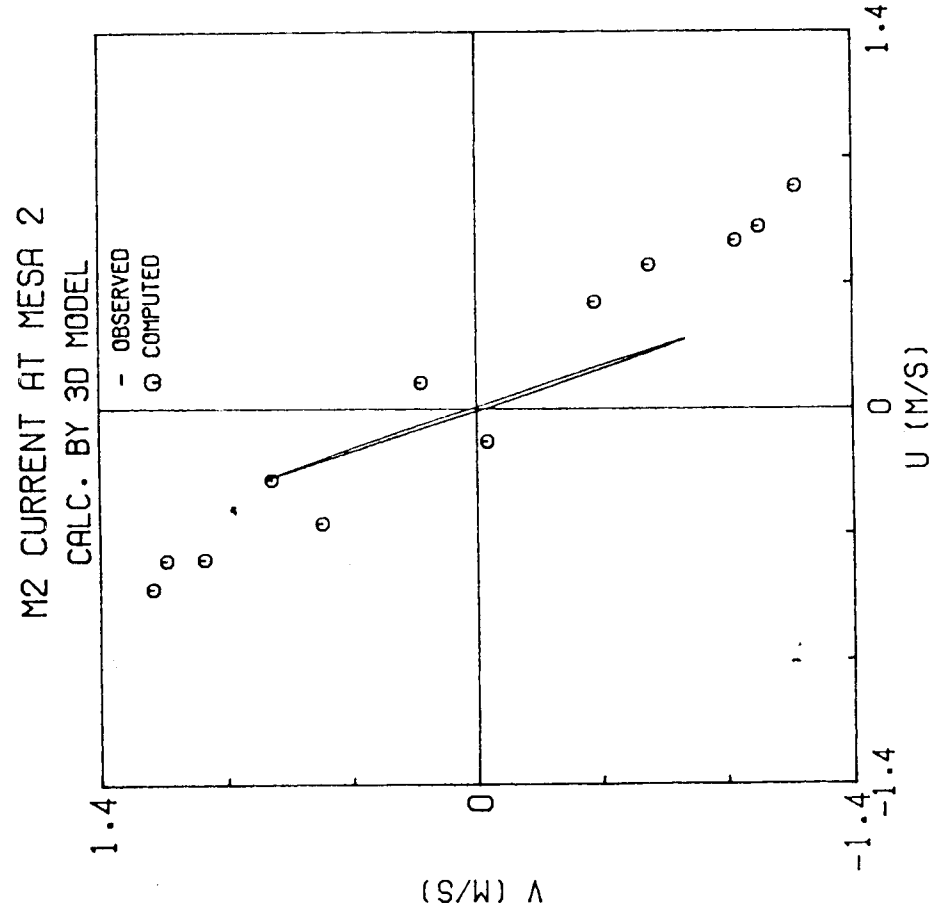
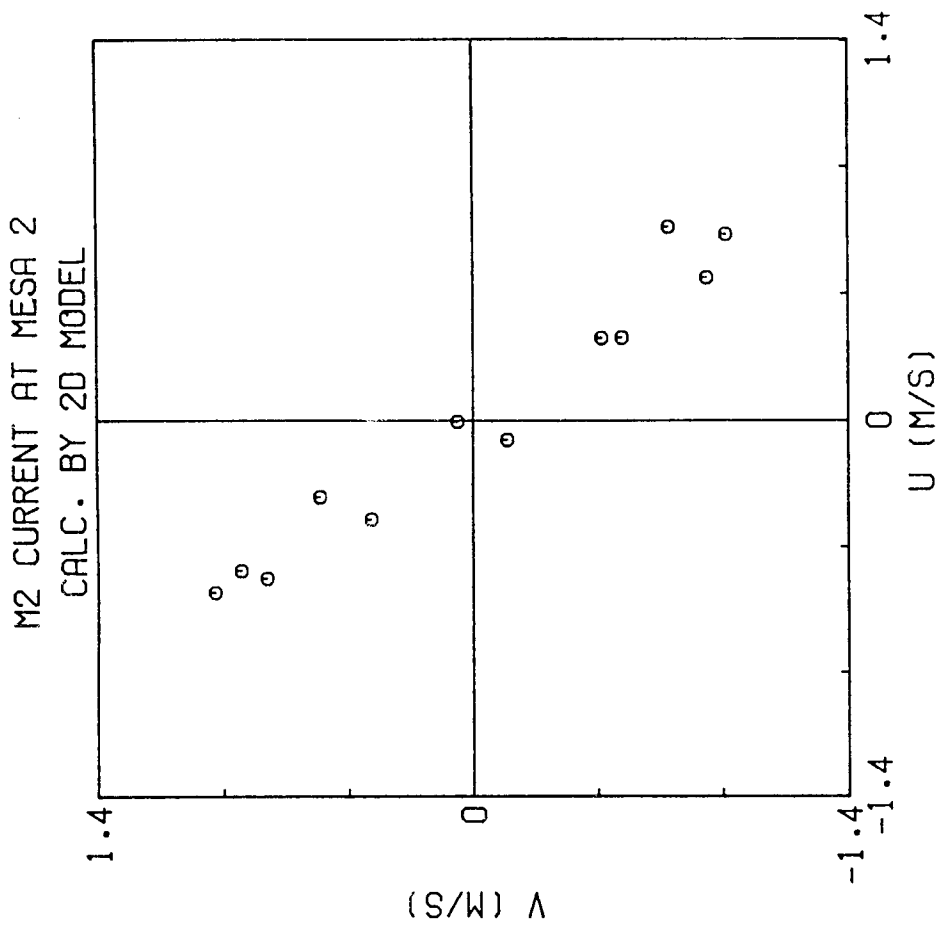


Figure 4.5a Comparison of Calculated and Observed M₂ Current Ellipses at MESA Station No. 2

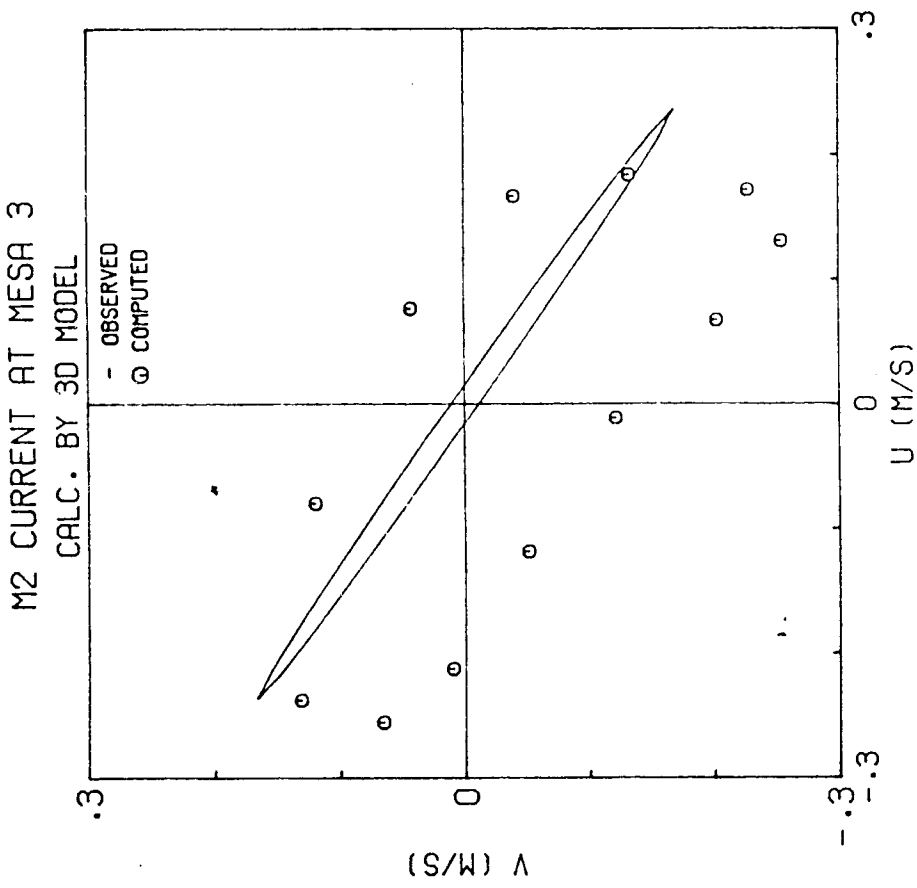
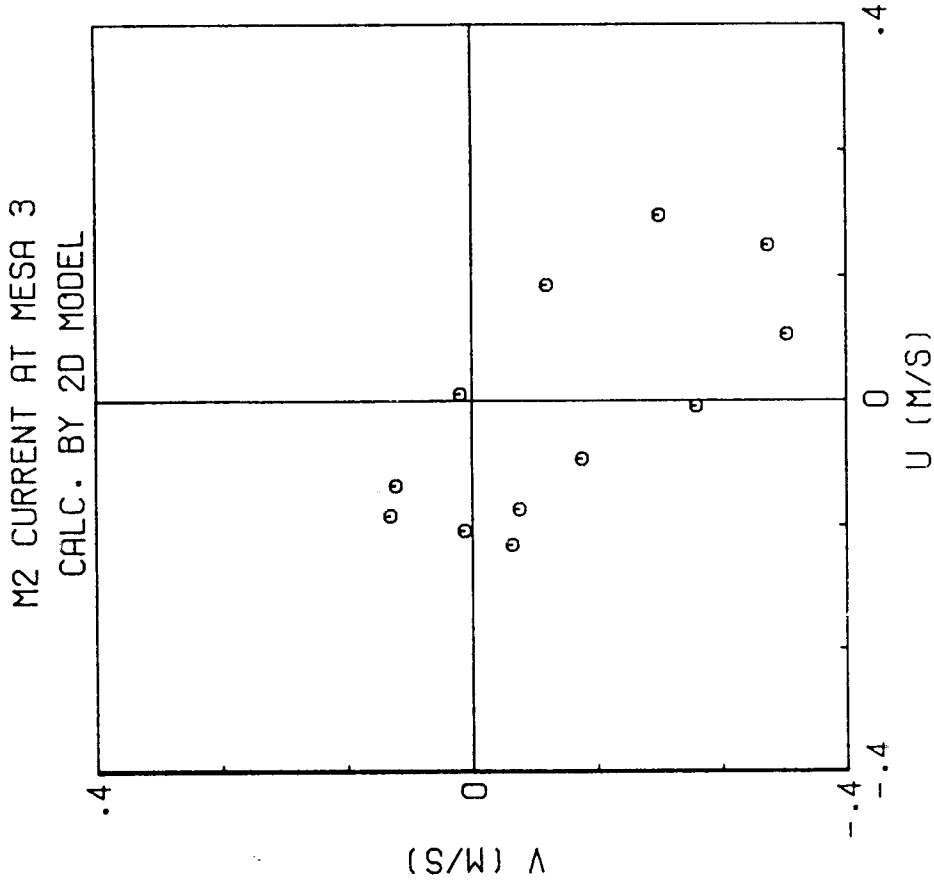


Figure 4.5b Comparison of Calculated and Observed M₂ Current Ellipses at MESA Station No. 3

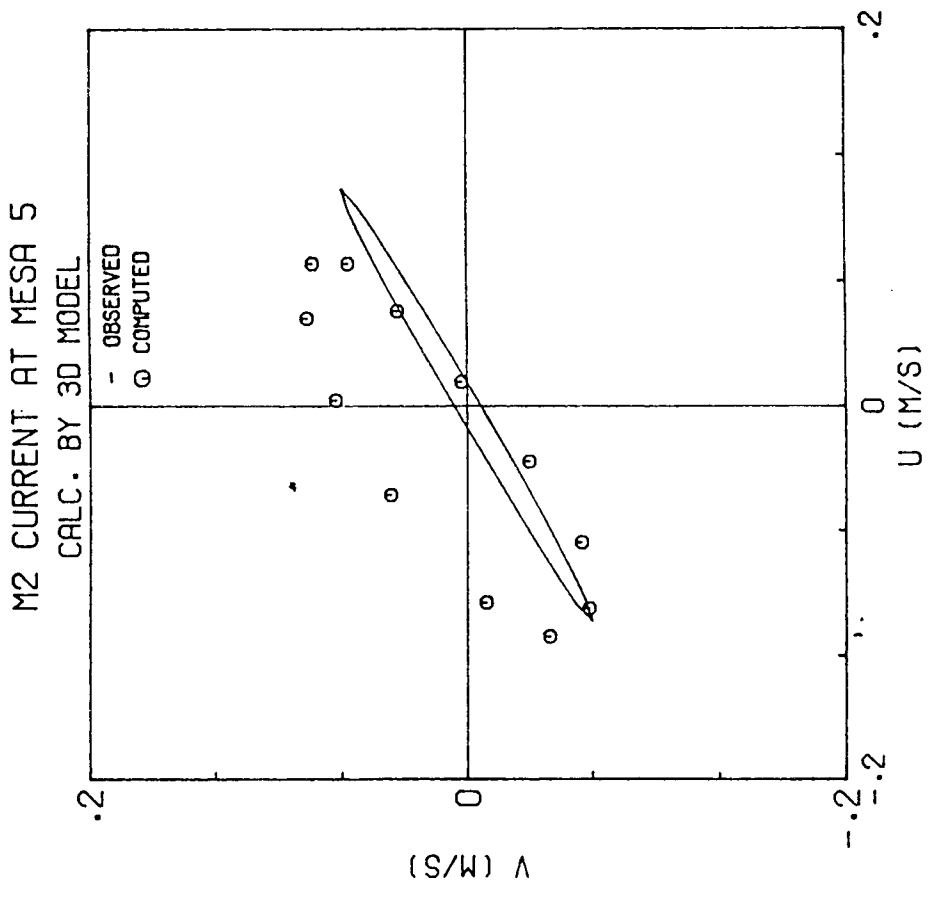
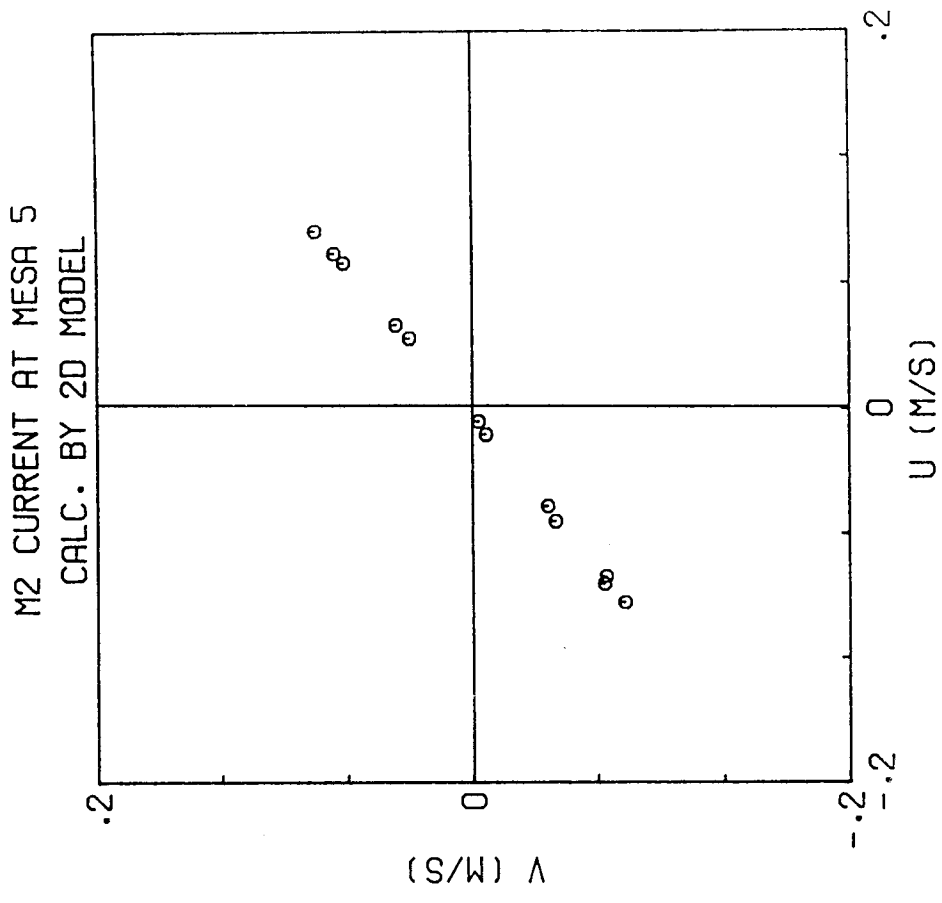


Figure 4.5c Comparison of Calculated and Observed M₂ Current Ellipses at MESA Station No. 5

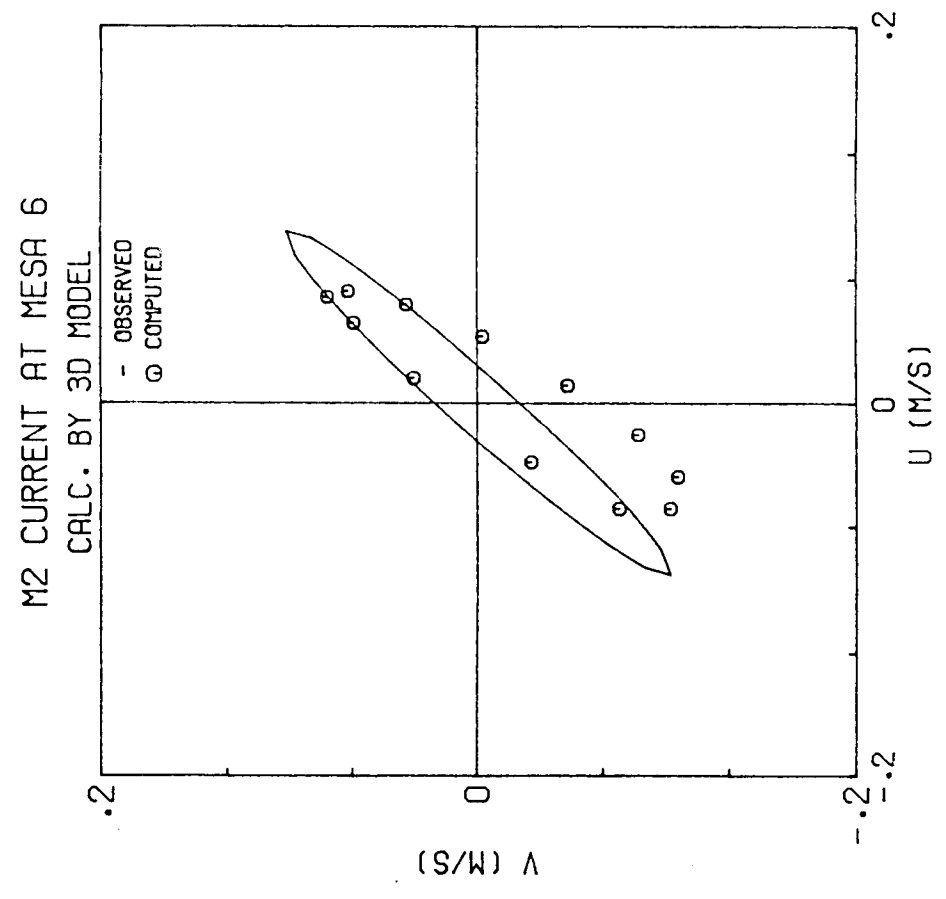
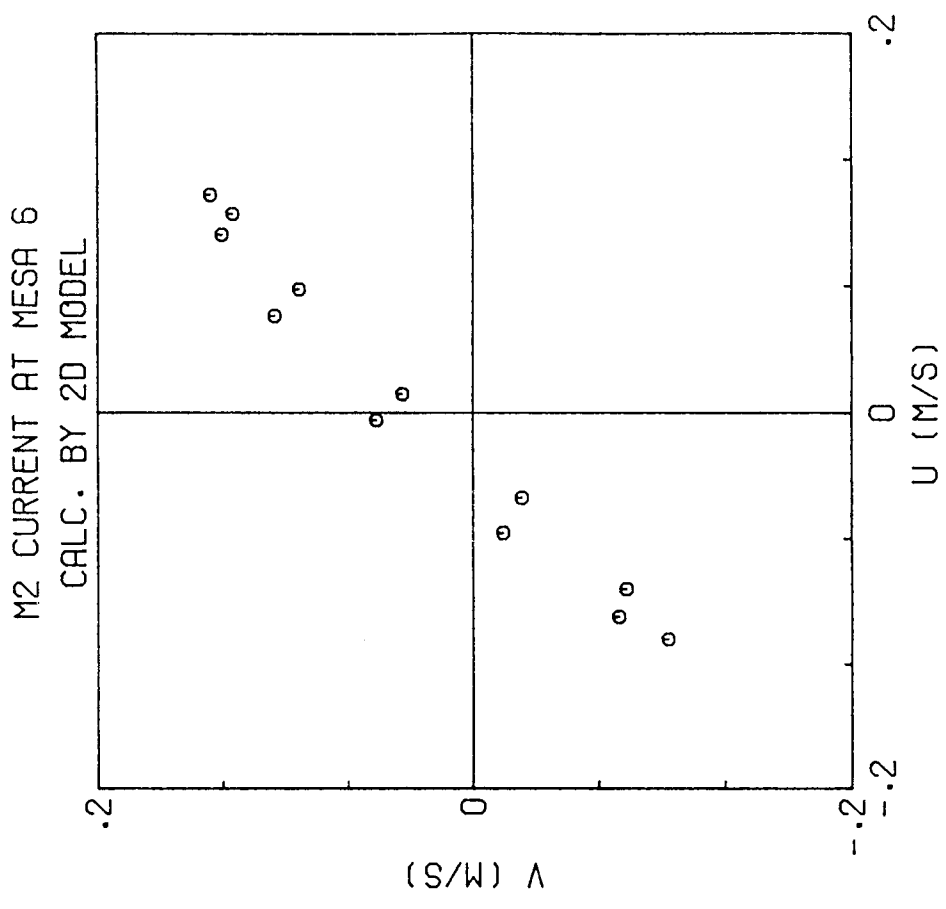


Figure 4.5d Comparison of Calculated and Observed M₂ Current Ellipses at MESA Station No. 6

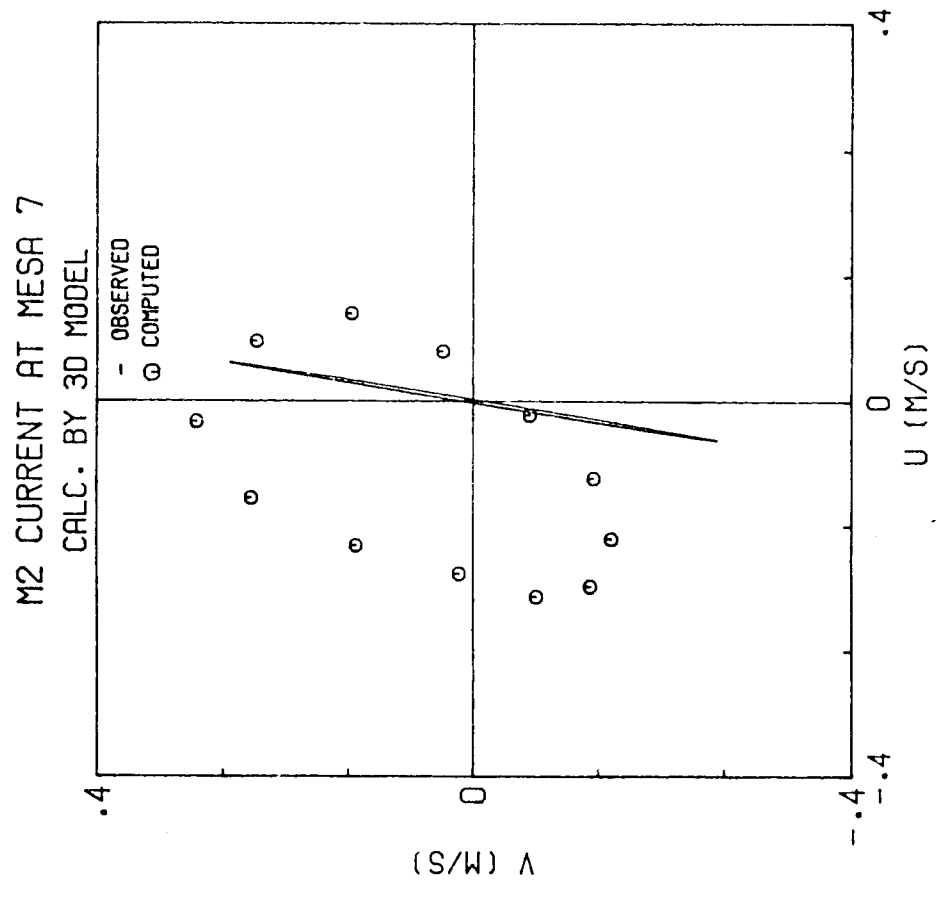
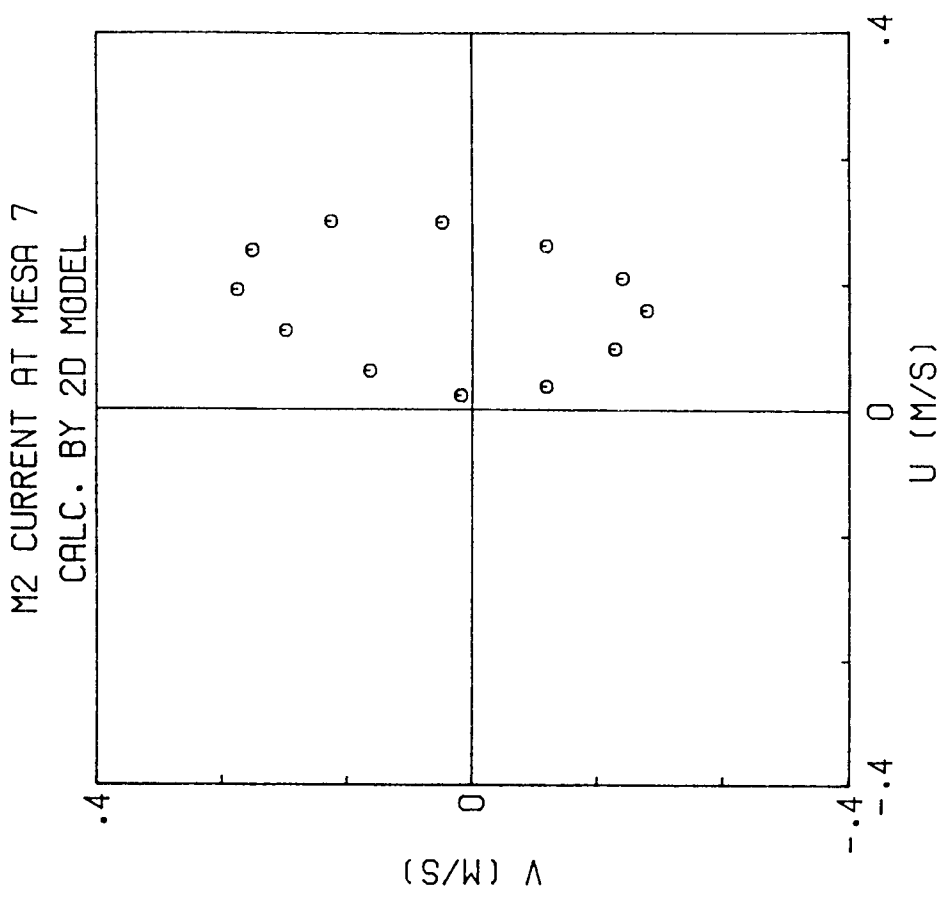
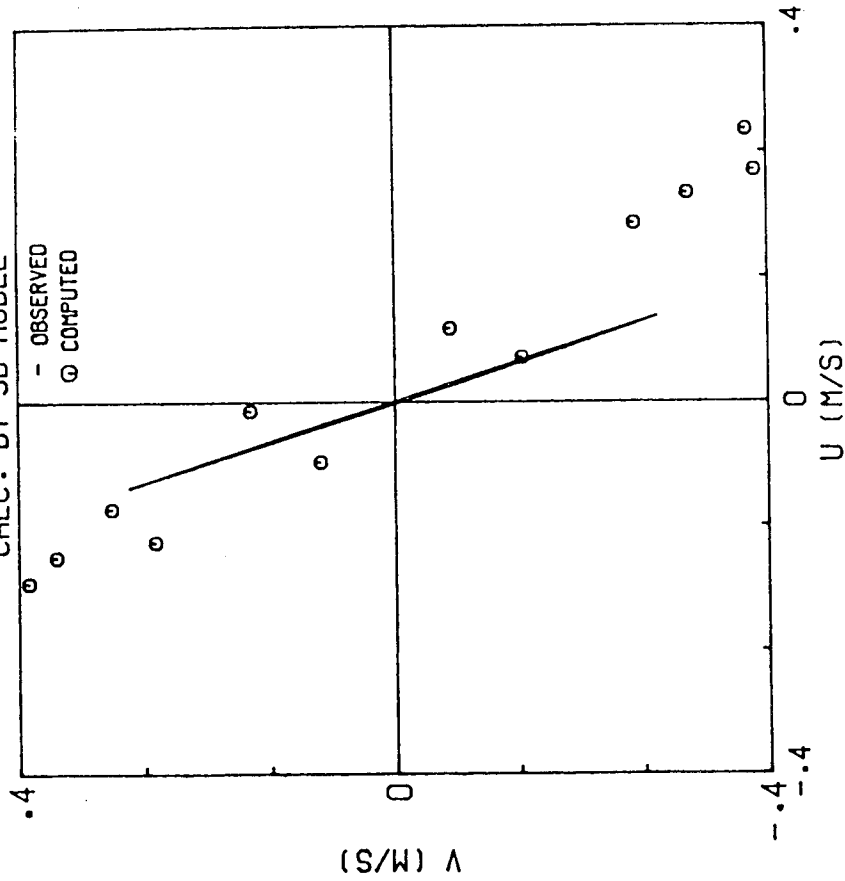


Figure 4.5e Comparison of Calculated and Observed M₂ Current Ellipses at MESA Station No. 7

K1 CURRENT AT MESA 2
CALC. BY 3D MODEL



K1 CURRENT AT MESA 2
CALC. BY 2D MODEL

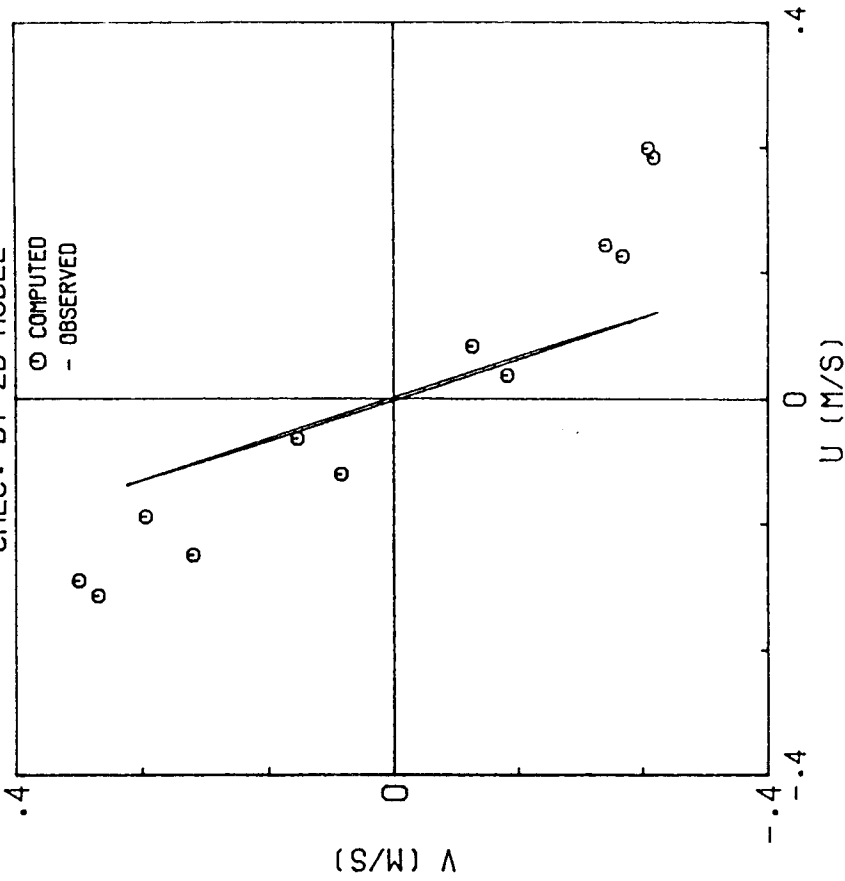
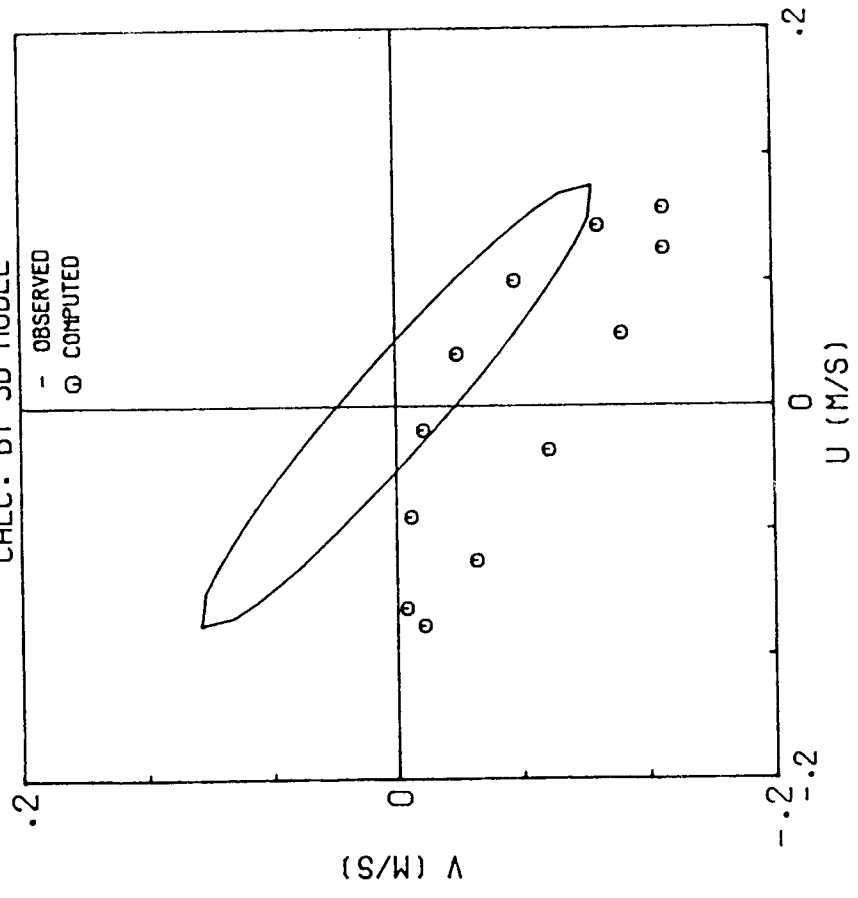


Figure 4.6a Comparison of Calculated and Observed K₁ Current Ellipses at MESA Station No. 2

K1 CURRENT AT MESA 3

CALC. BY 3D MODEL



K1 CURRENT AT MESA 3

CALC. BY 2D MODEL

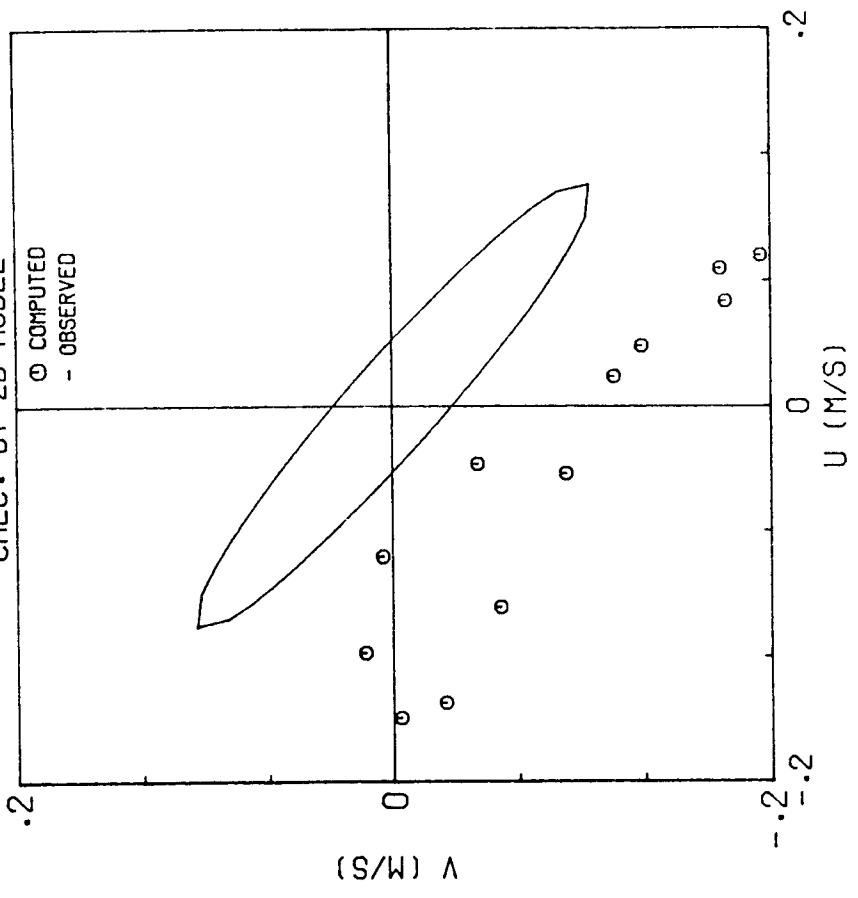


Figure 4.6b Comparison of Calculated and Observed K₁ Current Ellipses at MESA Station No. 3

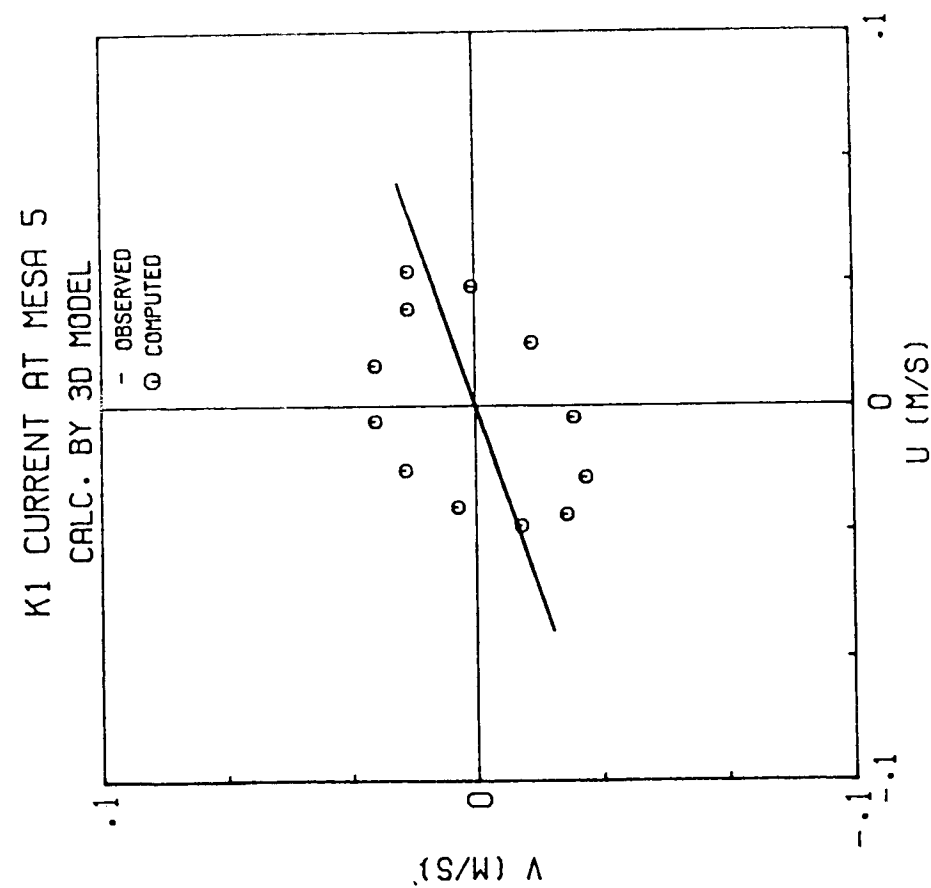
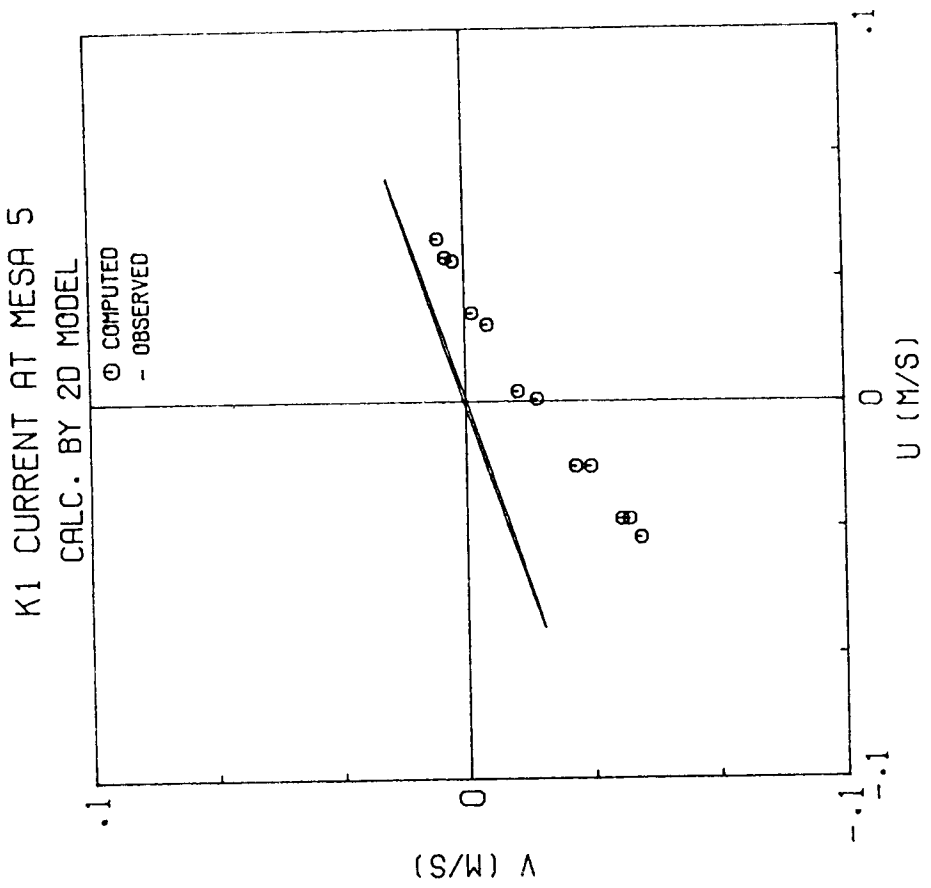


Figure 4.6c Comparison of Calculated and Observed K₁ Current Ellipses at MESA Station No. 5

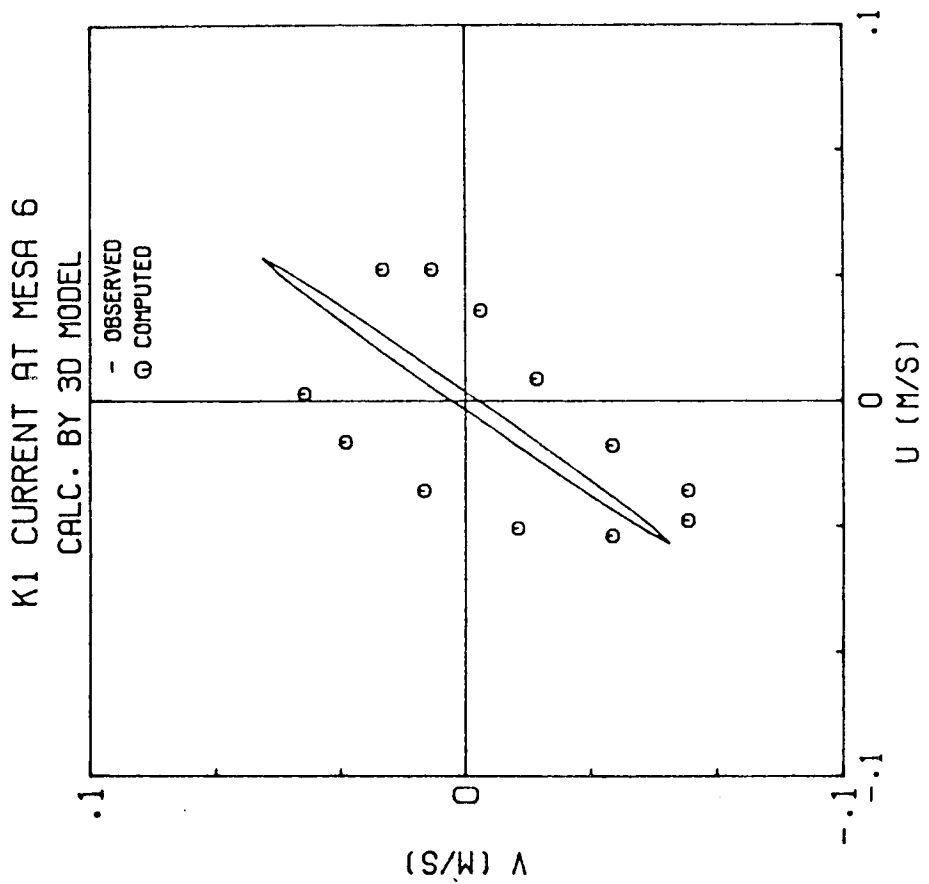
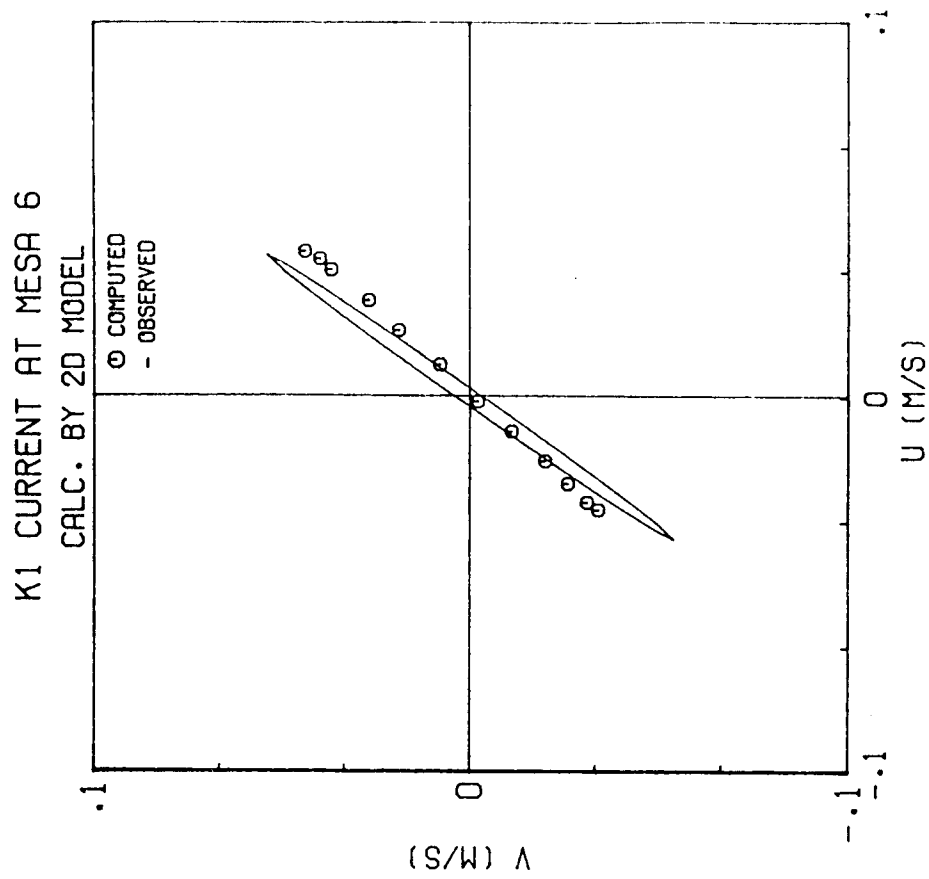


Figure 4.6d Comparison of Calculated and Observed K₁ Current Ellipses at MESA Station No. 6

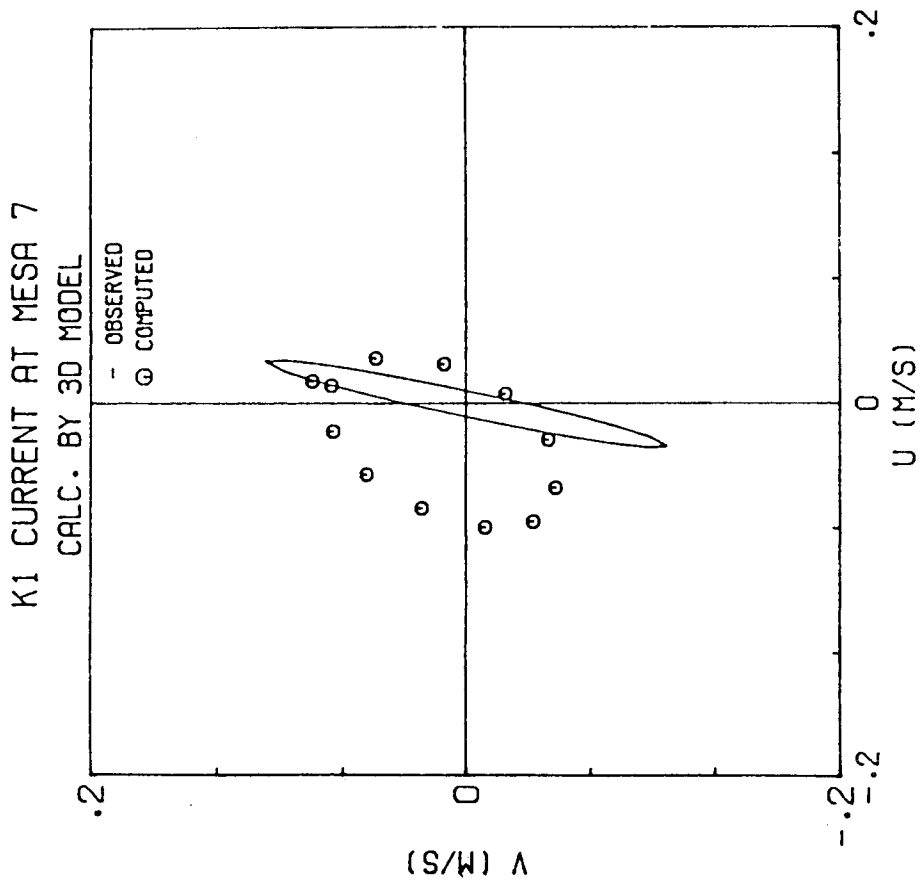
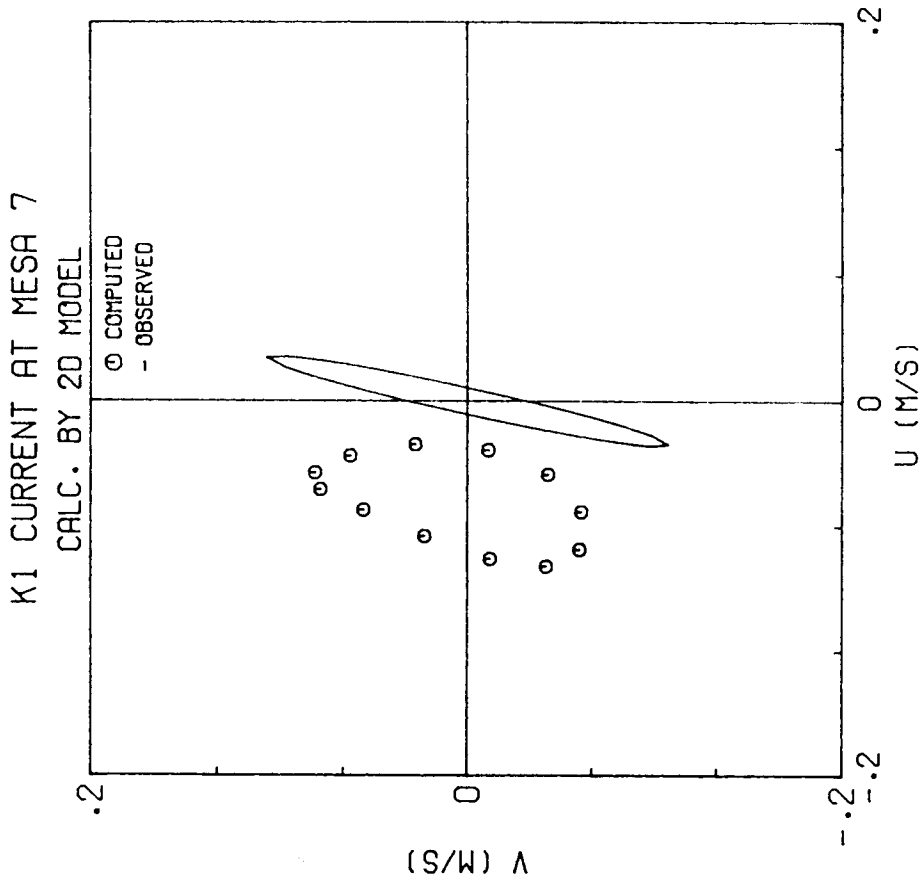


Figure 4.6e Comparison of Calculated and Observed K_1 Current Ellipses at MESA Station No. 7

Figures 4.5 and 4.6 show that the results from both models have captured the observed tidal current characteristics (magnitudes and directions) at most of the stations.

As expected, the calculated first layer tidal currents from the three-dimensional model and those from the depth-averaged model are quite different at the two deep water stations (Stations 5 and 6, both with depths between 175 and 185m). Due to the different formulations (particularly in nonlinear acceleration and momentum transport terms) and solution schemes (leap-frog versus implicit), the calculated first layer tidal current fields from the three-dimensional model always contain more eddies than those from the depth-averaged model throughout the deeper portion of Central Puget Sound. These eddies could not be verified by the present data set, but their presence could be one possible explanation for the wider current ellipses calculated by the three-dimensional model at Stations 5 and 6.

At Station 2 (in the Narrows at Tacoma), both models produced currents that were significantly stronger than the observation. There are two explanations for this phenomenon. The current measurement at this station was actually taken near the bottom of the channel (Mofjeld and Larsen, 1984) while the calculated currents are both depth averaged (there is only one layer over the Narrows for the three-dimensional model). Secondly, the chosen finite difference grid resolution near the station by both models actually straightened out the natural curvature of the channel at the Narrows (see Fig. 4.2) and therefore caused the increase in the calculated velocities.

Other stations at which more pronounced differences were displayed are Stations 3 and 7. The errors there again were thought to be the result of grid resolution over Dalco and Colvos Passages. The orthogonal grid system has created many "artificial" turns and sharp corners (steps stair) for the

otherwise fairly straight channels. Such turns and corners were necessitated by the chosen grid resolution and its orientation (chosen x-and y-axes). Although a different orientation might resolve these two passages better, it would have failed to represent other major portions of the central Puget Sound adequately. Available remedies for this particular difficulty include the use of 1) a more refined resolution in the present orthogonal grid system, 2) a curvilinear or irregular finite difference grid system, and 3) the finite element method. There are other computational problems associated with all of these options, but further discussion of them is beyond the scope of this study.

Analyses of data from several previous oceanographic studies (e.g., Geyer and Cannon, 1982; Bretschneider, et al., 1985) have long suggested the existence of a clockwise residual circulation around Vashon Island. One important task in the numerical experiments was to see if the results of the two models could verify this well-known observation.

Direct verification with the model results was not trivial. To examine the net circulation from the models, the M_2 residual currents at every computational node were first obtained by tidally averaging the tidal currents at every time step. The first layer M_2 residual current around Vashon Island calculated from the three-dimensional model results are shown in Fig. 4.7. Although the calculated residual current plot does show a clockwise circulation around Vashon Island, it is noticeable only in the center of the channel around Vashon Island. The current field shown in Fig. 4.7 revealed numerous eddies all around Vashon Island, especially along the shore represented by the "artificial corners" and stairsteps discussed earlier. The existence of these eddies could not be verified by any observation, but some of them were probably erroneously generated by the model due to the coarse

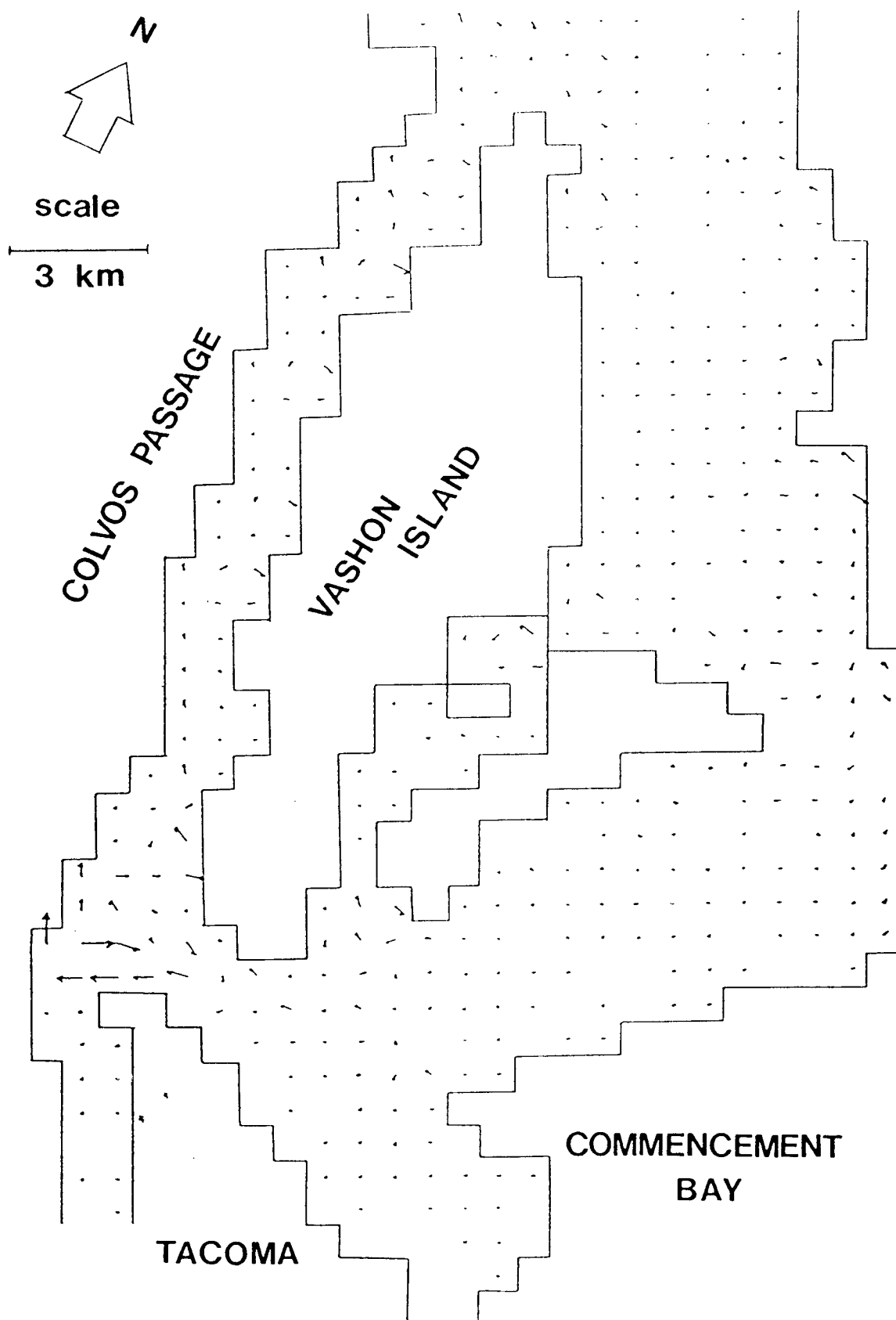


Figure 4.7 First Layer M_2 Residual Circulation Around Vashon Island Calculated from Three-Dimensional Model Results

resolution of the passage and channel geometry and the numerical scheme. Similar problem in other applications had been reported by Weare (1976) Pedersen (1986) and Smith and Cheng (1987).

Instead of using the two-dimensional current vectors to verify the net circulation, an effort was made to calculate cross-sectionally averaged currents (from the proper components of the vectors shown in Fig. 4.7) at 12 selected sections (all perpendicular to model x-and y-axis) around Vashon Island. These 12 sections are shown in Fig. 4.8. The calculated results from the two models are given in Tables 4.1 and 4.2. The directions of the cross-sectionally averaged residual currents in Tables 4.1 and 4.2 clearly show clockwise circulation around Vashon Island. In Table 4.1, the southward residual current component in the second layer of Section 1 is due to an abrupt shallow region just north of this section (between Neill Point and Gig Harbor). In Tables 4.1 and 4.2, the differences between the cross-sectionally averaged current magnitudes at some sections are due to the different velocity vector patterns calculated by the two models near those sections. In the absence of comparable data to verify them, the residual current field as shown Fig. 4.7 and the cross-sectionally averaged residual current magnitudes in Tables 4.1 and 4.2 should be carefully interpreted.

An 8000-step integration of the three-dimensional model (two layers and 77 x 39 horizontal nodes) with 50 smoothing operations requires about 20 System Resources Units (SRU) on a Cray X-MP/48 supercomputer. Because of the larger time step allowed, the single layer formulation, and the implicit numerical scheme used (an added advantage on vector processor machines), simulation of the depth-averaged model over the same time period requires only about a third of computing resources demanded by the three-dimensional model.

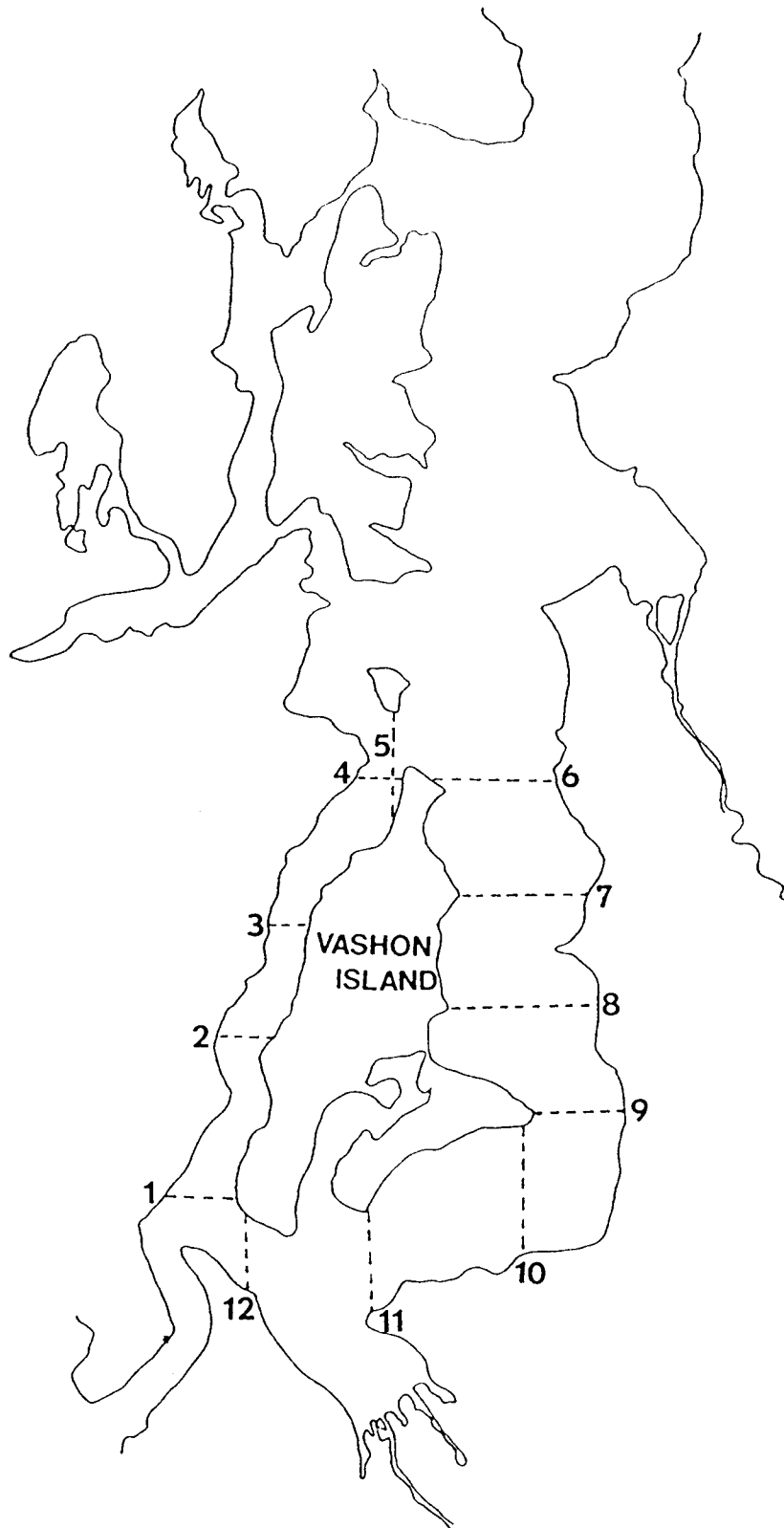


Figure 4.8 Selected Sections Around Vashon Island for Residual Circulation Calculation

TABLE 4.1 Cross-sectionally Averaged M_2 Residual Current Around Vashon Island Calculated from the 3D Model Results

Section (see Fig. 4.7)	First layer		Second layer	
	Magnitude* (m/sec)	Direction**	Magnitude (m/sec)	Direction
1	0.0622	N	-0.1170	S
2	0.0431	N	0.0297	N
3	0.0393	N	0.0360	N
4	0.0460	N	0.0406	N
5	0.0152	E	0.0353	E
6	-0.0123	S	-0.0074	S
7	-0.0065	S	-0.0041	S
8	-0.0143	S	-0.0168	S
9	-0.0199	S	-0.0111	S
10	-0.0022	W	-0.0075	W
11	-0.0131	W	-0.0170	W
12	-0.0392	W	-0.0387	W

*Positive and negative signs correspond to model x-and y- axis.

**N(North), S(South), E(East), and W(West) with respect to model x-y axes (model y-axis is to 350° Magnetic NOS Chart No. 18440).

Table 4.2 Cross-sectionally Averaged M_2 Residual Current Around Vashon Island Calculated from the Depth-Averaged Model Results

Section (See Fig. 4.7)	Magnitude* (m/sec)	Direction**
1	.0213	N
2	.0090	N
3	.0097	N
4	.0107	N
5	.0096	E
6	-.0103	S
7	-.0055	S
8	-.0068	S
9	-.0032	S
10	-.0040	W
11	-.0030	W
12	-.0073	W

*See Table 4.1 note

**See Table 4.2 note

CHAPTER 5

SUMMARY AND CONCLUSIONS

Management of the quality of Puget Sound water depends upon our improved ability to characterize the circulation and transport phenomena. Although some general knowledge of the flow physics has been developed from field observation and some simple models, detailed knowledge of the spatial and temporal variations of the hydrodynamics is still lacking. Multi-dimensional numerical hydrodynamics models are the most promising tools to facilitate improved understanding of the transport processes in Puget Sound. The development and evaluation of such models are urgently needed on Puget Sound research.

In this study, a depth-averaged and a layered three-dimensional hydrodynamics model were applied to a part of Puget Sound from Point Wells to the Narrows at Tacoma, referred to as Central Puget Sound in this study. The main objective of the modeling study was to evaluate the performance of the two models in characterizing the tidal hydrodynamics in the study area. Both models used a uniform horizontal resolution scale of 762m. The bathymetry and the vertical variation of the flow physics were represented by the three-dimensional model in two variable thickness layers. The boundary conditions for both models (M_2 and K_1 transports at Point Wells and The Narrows) were obtained from the results of a well-calibrated one-dimensional channel tide model from Pacific Marine Environmental Laboratory, NOAA.

Two types of comparison were made between the model results and observational data. For tidal characteristics, calculated and observed M_2 and K_1 tidal amplitudes and phases were compared at seven locations in Central Puget Sound. For the tidal currents, calculated and observed current ellipses for both the M_2 and K_1 constituents were compared at five stations in the

study area. Cross-sectionally averaged M_2 residual currents at 12 selected sections around Vashon Island were calculated from both models. The models' results show distinctive clockwise residual circulation patterns around Vashon Island, consistent with several analytical results derived from field observation.

In general, both numerical models have satisfactorily reproduced the observed tidal characteristics in Central Puget Sound. At the present resolution scale, the differences between the results of the two-layer three-dimensional (3-D) and the depth-averaged model are small, but the 3-D model requires about three times more computer resources to run.

With the horizontal resolution scale of 750m or more, the depth-averaged model can be used in the future to estimate basin-wide tide and tidal transport characteristics. One example of such application is the calculation of flushing (or exchange) between the urban embayments and the main basin of Puget Sound, an important parameter to be understood in the management of Puget Sound water quality. The depth-averaged model could also be used as a reference tool for planning future field studies or data acquisition activities.

For certain engineering and planning problems requiring more detailed knowledge of the current in the Sound such as treatment plant outfall siting, dredge material disposal, contaminant source identification, near surface and short term contaminants, etc., the use of the three dimensional model at smaller spatial resolution scales (250m to 100m horizontally and 5m to 50m vertically) is recommended. One viable approach to minimize computational demand at the initial stage would be to apply the 3-D model to a limited area or to selected urban embayments. The boundary conditions for such modeling attempts could be interpolated from the results of a coarse grid run. At such

smaller spatial and temporal scales, the effects of wind, river inflow, and perhaps density variations must be considered.

This study has suggested that with the availability of supercomputing resources, the complex tidal hydrodynamics of Puget Sound can be characterized in greater detail by sophisticated numerical models, and further application of the proposed (or other similar) models for Puget Sound water quality management is encouraged.

REFERENCES

- Abbott, M.B., Larsen J., and Tao J., 1985. "Modelling Circulations in Depth-Integrated Flows, Part I: The Accumulation of the Evidence", Journal of Hydraulic Research, 23:309-322.
- Bretschneider, D.E., Cannon G.A., Holbrook J.R., and Pashinski J.D., 1985. "Variability of Subtidal Current Structure in a Fjord Estuary: Puget Sound, Washington", Journal of Geophysical Research, 90(C6):11,949-11,958.
- Burns, R., 1985. The Shape and Form of Puget Sound, University of Washington Press, Seattle, WA, 100 pp.
- Cannon, G.A., Laird, N.P., and Keefer, T.L., 1979. "Puget Sound Circulation: Final Report of FY 77-78", NOAA Technical Memo EARL MESA-40, 55 pp.
- Chu, W-S., Yeh, W.W-G., and Kristof, R., 1981. "Mathematical Modeling and Parameter Identification in a Two-Dimensional Estuary: Case Study of the Hydraulic Model of San Francisco Bay and Delta", Water Resources Contribution No. 188, Water Resources Center, University of California, Davis, CA.
- Chu, W-S. and Yeh, W.W-G., 1985. "Calibration of a Two-Dimensional Hydrodynamics Model", Coastal Engineering, 9:93-307.
- Chu, W-S., Barker, B.L., and Akbar, A.M., 1988. "Modeling Tidal Transport in Arabian Gulf", to appear in the J. of Waterway, Port, Coastal and Ocean Engineering, ASCE, 114(4):455-471.
- Chu, W-S., 1988. "Remaining Problems in Practical Application of Numerical Models for Estuaries and Coastal Seas", Ch. 5, Coastal Modelling: Techniques and Application, ed. by V.C. Larkhan and A.S. Trenhaile, Elsevier, the Netherlands.
- Cokelet, E.D., Stewart, R.M., and Ebbesmeyer, C.C., 1984. "The Exchange of Water in Fjords: A Simple Model of Two Layer Advective Reaches Separated by Mixing Zones", Proc. of 19th Int'l Conf. on Coastal Engr. ASCE, New York, pp. 3124-3133.
- Collias, E.E., McGary N., and Barnes C.A., 1974. "Atlas of Physical and Chemical Properties of Puget Sound and Its Approaches", University of Washington Press, Seattle, Washington, pp. 235 .
- Downing, J., Eble M., Petillo A., and Roberts P., 1985. "Alki Wastewater Treatment Plant Outfall Improvements Predesign Study, Tch. Memo No. 8.2 Circulation and Effluent Transport", Municipality of Metropolitan Seattle, Washington.
- Dronkers, J.J., 1975. "Tidal Theory and Computations", in Advances in Hydroscience, 10, ed. by V.T. Chow, Academic Press, New York, N.Y., 145-230.
- Fischer, H.B., Editor, 1981. Transport Models in Inland and Coastal Waters, Academic Press, New York, N.Y.

- Geyer, W.R., and Cannon G.A., 1982. "Sill Processes Related to Deep Water Renewal in a Fjord", Journal of Geophysical Research, 87(101):7985-7996.
- Heaps, N.S. Editor, 1987: Three-Dimensional Coastal Ocean Models, American Geophysical Union, Washington, D.C., 208pp.
- Jamart, B.M., and Winter D.F., 1978. "A New Approach to the Computation of Tidal Motions in Estuaries", in Hydrodynamics of Estuaries and Fjords, ed. by J.C.J. Nihoul, Elsevier.
- Jamart, B.M., 1983. "Report on the Preliminary Modeling of Tides in East Passage", unpublished report to Municipality of Metropolitan Seattle, Washington.
- Killworth, P.D., 1984. "A Note on Smoothing Techniques for Leapfrog Time Integration Scheme", unpublished manuscript, Hooke Institute for Atmospheric Research, University of Oxford, Oxford, England.
- Kurihara, Y., 1965. "On the Use of Implicit and Interactive Methods for the Time Integration of the Wave Equation", Monthly Weather Review, 93(1):33-46.
- Lakhan, V.C., and Trenhaile, A.S. Editors, 1988. Coastal Modelling: Techniques and Applications, Elsevier Publisher, the Netherlands.
- Lavelle, J.W., 1987. "A Laterally Averaged Model of Admiralty Inlet and the Main Basin of Puget Sound", paper presented in the Workshop on Modeling Physical Oceanography of Puget Sound, Seattle, Washington, November 4-5.
- Leendertse, J.J., Alexander, R.C., and Liu, S-K., 1973. "A Three-Dimensional Model for Estuaries and Coastal Seas: Vol. I, Principles of Computation", R-1471-OWRR, Rand Corp., Santa Monica, California.
- Leendertse, J.J., and Liu, S-K., 1977. "A Three-Dimensional Model for Estuaries and Coastal Seas: Vol. IV, Turbulent Energy Computation", R-2178-OWRT, RAND Corp., Santa Monica, California.
- Leendertse, J.J., Langerak, A., and de Ras, M.A.M., 1981. "Two-Dimensional Tidal Models for the Delta Works", in Transport Models for Inland and Coastal Waters, edited by H.B. Fischer, 408-450, Academic Press, New York, NY.
- Liu, S-K., and Leendertse, J.J., 1978. "Multiple Dimensional Numerical Modeling of Estuaries and Coastal Seas", in Advances in Hydroscience, 11, ed. by V.T. Chow, Academic Press, New York, N.Y., 95-164.
- Messinger, J., and Arakawa, A., 1976. Numerical Methods Used in Atmospheric Models, GARP Publication No. 17, World Meteorological Organization, Geneva, Switzerland.
- Mofjeld, H.O., and Larsen, L.H., 1984. "Tides and Tidal Currents of the Inland Waters of Western Washington", NOAA Technical Memo ERL/PMEL-56, Seattle, Washington, 52 pp.

Mofjeld, H.O., 1987. "A Channel Model of Tides and Tidal Currents in Puget Sound" paper presented in the Workshop on Modeling Physical Oceanography of Puget Sound, Seattle, Washington, November 4-5.

Mofjeld, H.O., Lavelle, J.W., Walters, R.A., and Chu, W-S., Editors, 1987. "Abstracts of Workshop on Modeling Physical Oceanography of Puget Sound", Department of Civil Engineering, University of Washington, 33 pp.

Nakata, K., 1987. "The Three-Dimensional Numerical Model of Puget Sound", paper presented in the Workshop on Modeling Physical Oceanography of Puget Sound, Seattle, Washington, November 4-5.

Pedersen, G., 1986. "On the Effects of Irregular Boundaries in Finite Difference Models", Int'l Journal for Numerical Methods in Fluids, 6:497-505.

Puget Sound Water Quality Authority, 1987. "1987 Puget Sound Water Quality Management Plan", PSWQA, Seattle, Washington.

Richtmeyer, R.D. and K.W. Morton, 1967. Difference Methods for Initial Value Problems, 2nd Ed., Wiley Interscience, New York, NY, 206.

Roache, P., 1976. Computational Fluid Dynamics, Rev. Ed., Hermosa Publisher, Albuquerque, NM.

Schmalz, Jr., P.A., 1986. "A Numerical Investigation of Astronomic Tidal Circulation in Puget Sound", Misc. Paper CERC-86-9, U.S. Army Corps of Engineers, Vicksburg, Mississippi.

Smith, L.H., and Cheng, R.T., 1987. "Tidal and Tidally Averaged Circulation Characteristics of Suisun Bay, California", Water Resources Research, 23(1):143-155.

Water Resources Engineers, Inc., 1975. "Ecological Modeling of Puget Sound and Adjacent Waters", Report to the U.S. Environmental Protection Agency, Walnut Creek, California, 119 pp.

Weare, T.J., 1979. "Errors Arising From Irregular Boundaries in ADI Solutions of the Shallow-Water Equations", Int'l Journal for Numerical Methods in Engineering, 14:921-931.

Yeh, H.H., Chu, W-S., and Dahlberg, O., 1988. "Numerical Modeling of Separation Eddies in Shallow Waters", Water Resources Research, 24(4):607-614.